Applied Clay Science 212 (2021) 106218

Contents lists available at ScienceDirect

Applied Clay Science

journal homepage: www.elsevier.com/locate/clay

Research Paper

Optimisation of mortar with Mg-Al-Hydrotalcite as sustainable management strategy lead waste

Angélica Lozano-Lunar [a], José Ignacio Álvarez [b], Íñigo Navarro-Blasco [b], José Ramón Jiménez [a,*,1], José María Fernández-Rodriguez [c,1,*]

[a] Departamento de Ingeniería Rural, Escuela Politécnica Superior de Belmez, Universidad de Córdoba, Córdoba, Spain
[b] Departamento de Química, Facultad de Ciencias, Universidad de Navarra, Pamplona, Spain
[c] Departamento de Química Inorgánica e Ingeniería Química, Escuela Politécnica Superior de Belmez, Universidad de Córdoba, Córdoba, Spain

ARTICLE INFO

Keywords:
Hydrotalcite
Lead
Mortar
Calorimetry
Leaching
Waste management

ABSTRACT

This study analyses how a Mg-Al-Hydrotalcite with carbonate in the interlayer influences the hydration of mortar allowing the management of lead waste (solid or liquid) in a cement-based material. First, the compatibility of hydrotalcite with the cementitious matrix was studied through heat of hydration, workability, consistency, compressive strength and mineralogical phase formation. The changes produced by the incorporation of hydrotalcite were not drastic and the compatibility with the cement was verified. Lead was added in oxide and nitrate form to mortar with or without hydrotalcite and the same properties were evaluated, including a leaching test. The incorporation of lead delayed the hydration, this effect being increased by the hydrotalcite, which happened in the first instants of hydration. The addition of hydrotalcite counteracted the negative effect of lead in compressive strength values. The interaction between the hydrotalcite and the lead waste was favoured by the formation of plumbites under the pH conditions of cement hydration. Consequently, this interaction would seem to be superficial. The lead leaching decreased to values included in the "Non-Hazardous" limit of the environmental classification, very close to "Inert". All mortars were produced by two mixing procedures to establish differences. When hydrotalcite was included, the compressive strength was higher in the second procedure and lead leaching showed better behaviour in the first procedure. This research expands the possibilities of the management of solid and liquid waste contaminated with lead by using a Mg-Al-Hydrotalcite in cement-based matrices.

1. Introduction

Layered double hydroxides (LDH) are a group of clay minerals formed by positively charged layers and anions in the interlayer. These materials are also known as anionic clays, hydrotalcites or lamellar double hydroxides (Theiss et al., 2016). Generally they comprise the following structure: $[M^{2+}_{1-x}M^{3+}_{x}(OH)^{2}]^{x+}[A^{n-}_{x/n} \cdot mH_2O]^{x-}$, where M stands for a metal, divalent (Mg^{2+}, Mn^{2+}, Zn^{2+}, Ca^{2+}, etc.); or trivalent (Al^{3+}, Fe^{3+}, Cr^{3+}, etc.) and A represents an anion (CO_3^{2-}, NO_3^-, Cl^- and SO_4^{2-}) (Forano et al., 2006; Wu et al., 2018).

LDH have been widely investigated due to their variability in chemical composition exchange capacity and different surface values. Studies have focused on obtaining LDH through different synthesis procedures such as coprecipitation (Cao et al., 2018; González et al., 2015; Otero et al., 2012; Pérez et al., 2017; Pérez et al., 2007; Pérez et al., 2012), ion exchange (Pérez et al., 2007; Pérez et al., 2012; Rouahna et al., 2018) or calcination and rehydration process (Otero et al., 2013; Pérez et al., 2017). In addition, these materials are used in various applications such as adsorption of pesticides, medical antacids, drug administrators, motor lubricants, catalysts, etc. (Li and Duan, 2006; Otero et al., 2013; Otero et al., 2012; Pérez et al., 2017; Theiss et al., 2016; Wang and O'Hare, 2012).

Due to their versatility, low cost and compatibility with cementitious materials (Hongo et al., 2017), LDH have begun to be used as active

* Corresponding authors at: Departamento de Química Inorgánica e Ingeniería Química, Instituto Universitario de Nanoquímica (IUNAN), Facultad de Ciencias, Universidad de Córdoba, Campus de Rabanales, Edificio Marie Curie, E-14071 Córdoba, Spain (José María Fernández). Departamento de Ingeniería Rural, Universidad de Córdoba, Ed. Leonardo Da Vinci, Campus de Rabanales, Ctra. N-IV, km-396, CP 14014 Córdoba, Spain (José Ramón Jiménez).
E-mail addresses: jrjimenez@uco.es (J.R. Jiménez), um1feroj@uco.es (J.M. Fernández-Rodriguez).
[1] Both authors equally contributed to the paper.

https://doi.org/10.1016/j.clay.2021.106218
Received 16 March 2021; Received in revised form 27 May 2021; Accepted 14 July 2021
Available online 21 July 2021

components in cement to modify some aspects of mortars (Yang et al., 2015). In their fresh state, calcined Mg-Al-LDH have accelerated the setting and hardening of cement pastes compared to the reference paste (Ke et al., 2016). Regarding their mechanical behaviour, authors such as Wu et al. (2018) stated that a 3% addition of calcined Mg-Al-LDH improved the compressive strength at an early age (3 days) to around 40% compared to the paste without hydrotalcite content. This fact was due to the incorporation of a LDH crystal seed (very small size) which reduced the barrier energy of the precipitation of hydration products accelerating the hydration of cement (Shao et al., 2001; Xu et al., 2009). However, in the research carried out by Cao et al. (2018) compressive strengths in cementitious slurries at early ages (1, 3 and 7 days) were slightly reduced with the Ca-Al-LDH incorporation in percentages of 0.025% and 0.05% of the weight of the cement. Due to the crystal seed of Ca-Al-LDH there was a strong effect on the reaction of C_3A that inhibited the C_3S reaction generating a slow evolution of early strength. Yang et al. (2015) recorded that compressive strength values at 28 days decreased approximately 17% with a 10% incorporation of hydrotalcite modified with p-aminobenzoate in the interlayer, probably due to cement replacement of LDH. The durability aspects of cement pastes such as chloride penetration or carbonation depth were also improved with the incorporation of hydrotalcites (Shui et al., 2018; Yoon et al., 2014).

Despite the multitude of practical applications, research on the interaction between different LDH and cement-based materials, as well as their influence on the properties of pastes/mortars/concretes, is still relatively insufficient (Cao et al., 2018; Wu et al., 2018). Therefore, one of the aims of this research was to focus on the interaction between LDH and cementitious materials, using a non-calcined LDH of Mg and Al and carbonate in the interlayer (named HT).

Another major hydrotalcite use has been as a heavy metal adsorbent, capturing in the interlayer contaminants in soil and aqueous medium (Gasser et al., 2016; Inacio et al., 2001; Otero et al., 2013; Otero et al., 2012; Pérez et al., 2017; Villa et al., 1999). Lead is a heavy metal recognised as highly hazardous for ecosystems and human health (Mol, 2011). In addition, its low degradability generates bioaccumulation in living systems (Katsioti et al., 2008). Authors such as González et al. (2014, 2015) achieved lead capture in an aqueous medium through different LDH.

Solid industrial waste with lead content must be deposited safely in landfill by pre-treating. Stabilisation/Solidification (S/S) techniques using cement-based materials have traditionally been used for the pre-treatment of solid waste with high heavy metal load (Pensaert et al., 2008). Waste, such as cutlery (Belebchouche et al., 2015; Chaabane et al., 2017), batteries (De Angelis et al., 2002), sewage sludge (Katsioti et al., 2008)or electric arc furnace dust (Lozano-Lunar et al., 2019b) has been satisfactorily managed through S/S. This technique allows the generation of cementitious monoliths, with enough chemical and physical integrity for landfill. The criteria to verify the effectiveness of the S/S technique meet the needs of the mechanical strength registered by the monoliths and the behaviour, in monolithic and/or granular state, of metal liberation by leaching tests (Ledesma et al., 2017).

Sometimes the monoliths are not satisfactory due to low mechanical strength. Ledesma et al. (2018) studied the S/S of two types of waste with a high content of heavy metals using a ratio of 2:1 (mortar:waste). These authors observed that the mortars produced with one type of waste did not obtain mechanical strengths greater than 1 MPa, because its high metal content and its natural pH values did not allow a common cement hydration. It is known that heavy metals interfere in the hydration and microstructure of the cementitious pastes. In most of the cement hydration studies with Zn, a delay in setting time was reported. This fact is usually associated with the formation of a protective coat on the cement grains which hinder hydration (Asavapisit et al., 2005; Yousuf et al., 1995). Most authors agree that the most relevant phase in this process was Calcium Zincate ($CaZn_2(OH)_6{\cdot}2H_2O$) formed during the hydration of the cement (Chen et al., 2009; Fares et al., 2016; Gineys et al., 2010; Weeks et al., 2008).

Other metals such as Pb or Cr give rise to different effects depending on their oxidation state. In this regard, Nestle (2004) observed a delay in the hydration of the pastes with PbO and a lesser impact on pastes with $Pb(NO_3)_2$ and Pb_3O_4 content. However, PbO_2 had no relevant incidence. The delay due to the incorporation of PbO was attributed to the partial dissolution of PbO. This statement is in accordance with the PbO hydrolysis giving rise to the formation of plumbites (PbO_2^{2-}) (Weeks et al., 2008).

Wang and Vipulanandan (2000) recorded an inhibition of cement hydration when Cr^{6+} (K_2CrO_4) reacted with Ca^{2+}, decreasing the formation of Portlandite ($Ca(OH)_2$) (Jain and Garg, 2008). However, in the study carried out by Lasheras-Zubiate et al. (2012) with Cr^{6+} ($K_2Cr_2O_7$) an acceleration of the hydration of cement pastes was recorded. Meanwhile, Otomoso et al. (1995) analysed the influence of Cr^{4+} on tricalcium silicate, concluding that it had no effect on its hydration. Regarding Cr^{3+}, authors such as Fernández Olmo et al. (2001) and Sinyoung et al. (2011) reported a delay in the setting of cement pastes as a function of the percentage of Cr_2O_3 incorporated in the mix, relating it to a delay in the hydration of tricalcium silicate and aluminates (Chen et al., 2007).

Although S/S is especially suitable for pre-treating waste with heavy metals, not all are immobilised correctly, such as lead. Navarro et al. (2011) experienced problems in the lead S/S with cement-based mortars due to the high mobility of this metal in alkaline medium reached during the cementitious mortar hydration. Therefore, it is the high metal release that prevents landfilling of waste treated with S/S (Navarro et al., 2011).

A relatively unexplored way to manage waste with lead content is the combination of LDH and cementitious matrices. This technique was named as Double Barrier Technique (DBT) in a previous study carried out by Lozano-Lunar et al. (2019a), where it was possible to control the lead release by adding LDH with *meso*-2,3-dimercaptosuccinic acid (DMSA) in the interlayer to cementitious mortars. These mortars reduced the lead release by approximately 50% compared to mortar without hydrotalcite content (from 20.29 mg/kg to 9.88 mg/kg). A similar technique was used by the authors Lasheras-Zubiate et al. (2011) who introduced chitosan into mortars doped with heavy metals (Cr, Pb y Zn). They achieved up to a 99.6% reduction in lead release by introducing chitosan into the cementitious matrices compared to the polymer free mortar.

The effect of Mg-Al-Hydrotalcite in cementitious matrices on solid and liquid lead waste management optimisation were analysed. First, the compatibility between the hydrotalcite and the mortar was assessed for their fresh and hardened state properties. The properties' heat of hydration, workability, consistency, compressive strength and mineralogical phase formation were analysed. Secondly, lead was added in oxide and nitrate form to mortar with hydrotalcite and the physical-mechanical properties were analysed. Leaching studies were included too. The interaction between Mg-Al-Hydrotalcite and lead was possible due to the formation of plumbites in the alkaline environment of cement hydration. This research intends to expand the possibilities of management solid and liquid waste contaminated with lead by using hydrotalcite in cement-based matrices.

2. Materials and methods

2.1. Material characterisation

The mortars were produced with cement, siliceous filler, natural sand, lead oxide, lead nitrate and hydrotalcite with carbonate in the interlayer.

The cement CEMI/52.5 R (C), according to JOINS IN 80303–1 and JOINS IN 197–1 (AENOR, 2019), was supplied by Votorantim Cimentos S.A. The siliceous filler (SF) and the siliceous natural sand (NS) come from Lorda and Roig S.A. and Áridos Álvarez (Córdoba), respectively.

The PbO, $Pb(NO_3)_2$ and the hydrotalcite with carbonate (HT) were provided by Sigma-Aldrich.

The chemical composition of C was provided by the manufacturer. The chemical composition of SF and NS was determined by X-ray energy dispersion analysis (EDAX) connected to a Jeol JSM-6300 scanning electron microscope using an acceleration potential of 20 KV and 15 mm. Table 1 shows the chemical composition of C, SF and NS. C shows, as major oxides, the CaO and SiO_2 and to a minor extent Al_2O_3. It can be observed that SF and NS have siliceous composition. In NS there are some minority oxides such as Al_2O_3, Fe_2O_3 and CaO. The hydrotalcite was composed of Mg and Al in the layer, while CO_3^{2-} occupied the interlayer. The hydrotalcite composition, according to the provider, was as follows: $Mg_6Al_2(CO_3)(OH)_{16}.4H_2O$.

The particle size distribution of C, SF and HT in volume percentage was determined in a Mastersizer S analyser (Malvern Instruments) using ethanol as dispersant. The particle size distribution of C, SF and HT is represented in Fig. 1. C and SF exhibit a distribution with particle sizes oscillating between 0.06 and 100 μm showing a small percentage of particles around 0.3 μm being more relevant in C. The largest percentage of particles in both materials was observed around 20 μm. This percentage was higher in SF. HT showed a bimodal particle size distribution with two maximums around 0.5 and 3 μm. The particle size distribution of NS was calculated in accordance with UNE-EN 933–1:2012 (AENOR, 2019). Fig. 2 reflects the particle size distribution of NS, as well as a 2 mm maximum size, according to UNE-EN 933–2:1996 (AENOR, 2019).

The mineralogical composition of C, SF and NS and HT was studied by X-ray diffraction (XRD). NS was crushed and sieved through a 0.125 mm sieve and an instrument Bruker D8 Discover A25 with Cu-Kα radiation was used. By scanning from 5° to 80° (2θ) at a speed of $0.02°2\theta{\cdot}s^{-1}$, the diffraction patterns of these materials were obtained. The XRD patterns of C, SF, NS and HT are shown in Fig. 3. The tricalcium silicate (Ca_3SiO_5; 42–0551) (JCPD, 1995) and dicalcium silicate (Ca_2SiO_4; 24–0034) (JCPD, 1995) were the main phases in C and Gypsum ($CaSO_4{\cdot}H_2O$; 33–0311) (JCPD, 1995) was also detected. The silica oxide (SiO_2; 33–1161) (JCPD, 1995) was the only phase registered in SF. NS was mostly composed of silica oxide (SiO_2; 33–1161) (JCPD, 1995) and small amounts of calcium carbonate ($CaCO_3$; 05–0586) (JCPD, 1995). HT showed an XRD pattern that corresponds to the hydrotalcite of Mg and Al with carbonate in the interlayer ($Mg_6Al_2(CO_3)(OH)_{16}{\cdot}4H_2O$; 14–0191) (JCPD, 1995).

2.2. Experimental design

First of all, the effect of the HT addition on the fresh and hardened properties of mortars was analysed. From the reference mortar (M0) dosage HT was added in the following amounts: 15, 30, 60 and 120 g, which represented the following percentages by weight compared to cement: 1.25%, 2.5%, 5% and 10%. Mortars with HT addition were named as M15, M30, M60 and M120. Fresh and hardened state properties were evaluated. M120 was selected to analyse the effect of HT in cementitious matrices with solid and liquid lead waste.

In order to study the effect of lead waste in cementitious matrices two amounts of lead were used (13 g for mortars with PbO and 19 g for mortars with $Pb(NO_3)_2$), named MPb and MPbN. Lead was incorporated as a replacement of SF in weight. Lead incorporation to the mortars was added according to the mixing procedure, explained in the following section.

To analyse the effect of HT in cementitious matrices on solid and liquid lead waste management optimisation. Two mortars with 120 g of HT, and PbO or $Pb(NO_3)_2$ were produced, named as M120Pb y M120PbN. Fresh and hardened state properties were analysed. In addition, lead mobility, in its two chemical forms, was analysed by leaching tests in a monolithic state. M0 was also evaluated in order to verify its inert classification.

The nomenclature and dosage of the mixes are shown in Table 2.

Table 1
Chemical composition of cement (C), siliceous filler (SF) and natural sand (NS).

Oxides	C*	SF**	NS**
Fe_2O_3	2.59	–	6.80
CaO	64.58	–	4.73
SiO_2	20.16	100	72.14
SO_3	3.46	–	–
K_2O	1.00	–	2.53
MgO	0.98	–	0.70
Al_2O_3	4.52	–	10.31
Loss of ignition (L.O.I.)	2.84	–	–

* Data provided by manufacturer.
** Composition determined with EDAX.

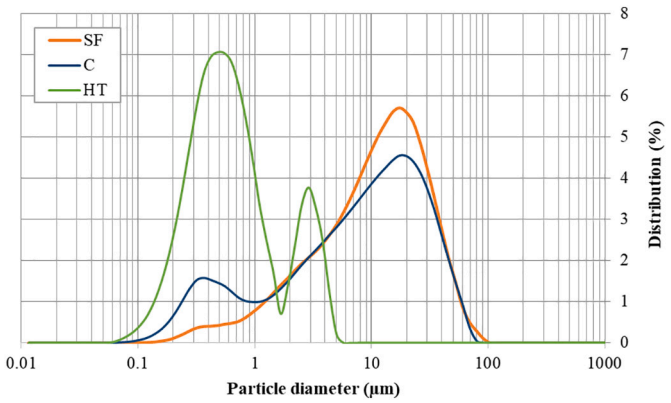

Fig. 1. C and SF particle-size distribution.

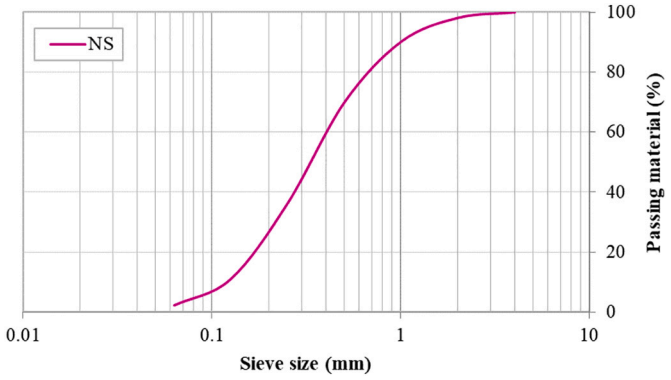

Fig. 2. NS particle-size distribution.

2.3. Mixing procedure

Two families of mortars were produced through two different mixing procedures (MProc-A and MProc-B). Each family consisted of 9 mixes (Table 2). Both families were produced with constant water/cement ratio (w/c) of 0.70. The w/c ratio was experimentally established to guarantee the correct handling of the mixes.

The mixing procedure A (MProc-A) consisted of adding, in a period of 3 min, water, C, SF, lead salts in powdery solids, HT and NS, as appropriate, at a speed of 140 ± 5 min^{-1}. After the incorporation of all the constituents, the mixing was continued for 2 min at a higher speed 285 ± 10 min^{-1} (Fig. 4a). The mixing procedure B (MProc-B) had been designed to analyse the possible remediation of aqueous medium contaminated with lead using them as mortar mixing water. First, an interaction between lead and HT was carried out (Fujii et al., 1992; Liang et al., 2013). To do so, the lead was dissolved in tap water and. This solution was placed in a tumbler. Subsequently, HT was

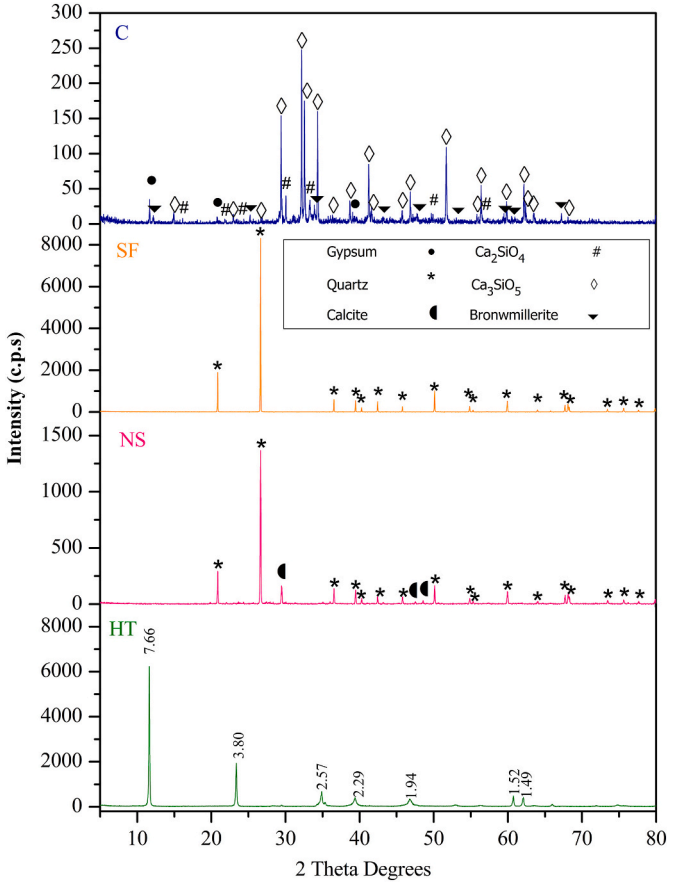

Fig. 3. XRD patterns of cement (C), siliceous filler (SF), natural sand (NS) and hydrotalcite (HT).

incorporated into the solution for 48 h. Then this mix was used as mixing water for the mortars and the mixing procedure continued equal to MProc-A. The mixing procedure B is shown in Fig. 4b.

The interaction between lead and HT was studied with an isotherm. This experiment was carried out under environmental conditions. A total of 11 interaction points was experimented on with a constant HT amount equal to 3.57 g and a volume of 25 mL added. The desired lead concentrations in the solution corresponded to the following percentages: 0%, 1%, 3%, 7%, 9%, 11%, 13%, 15%, 20%, 25% and 30% compared to HT weight. The interaction experiment was carried out using $Pb(NO_3)_2$, since the PbO is a product with low solubility in water and its incorporation was related to the S/S of solid waste with lead content. The mix of HT, $Pb(NO_3)_2$ and water was homogenised by magnetic stirring for 4 h, guaranteeing contact of HT with lead. Then the solid and liquid phase was separated by centrifugation at 8000 rpm for 15 min in polyethylene tubes. An eluate was filtered using a 0.45 μm filter. Subsequently, dilutions of each point were prepared according to the calibration line of the equipment used for the lead measurement. The lead concentration was determined by atomic absorption spectrophotometry using a Perkin Elmer AAnalyst 800 device.

The M0 was mixed by MProc-A since this mortar did not incorporate HT or lead in its composition, the preparation of mixing water was not necessary and could not be mixed using MProc-B.

10 cylindrical specimens (40 mm of diameter and 80 mm of height) were manufactured from each of the dosages and they were stored in a climatic chamber at a relative humidity of 95% ± 5% and a temperature of 20 °C ± 2 °C for 28 days.

2.4. Fresh state properties of mortars

In fresh state, the mortar hydration degree was evaluated through the heat of hydration. The hardening of the mortars is based on the hydration reaction of the cement with water. This reaction produces heat, which, when released in this reaction is proportional to the mortar hydration degree and can be correlated with the setting time. For this reason, a study of heat of hydration versus time was carried out on all mortars (MProc-A and MProc-B) to analyse the influence of HT, PbO and $Pb(NO_3)_2$ and their combined effect on the mortar setting. The evolution curves of the heat of hydration of the mortars were determined using an isothermal air conduction calorimeter TAM Air. In addition, the workability and consistency (flow table values) properties were measured in accordance with the UNE-EN 1015–9:2000 (AENOR, 2019) and UNE-EN 1015–3:2000 (AENOR, 2019).

The workability time according to UNE-EN 1015–9:2000 (AENOR, 2019) is the period between the contact of water with the cement up to a penetration strength value of 0.5 N/mm^2. A maximum of five penetrations were carried out per mortar fresh sample by a penetrometer. The penetration strength calculation was determined by interpolation of the immediate upper and lower values to 0.5 N/mm^2. The workability time of the mortars corresponds to the average of 3 repetitions.

After the mixing procedure, mortar consistency (flow table values) was evaluated according to UNE-EN 1015–3:2000 (AENOR, 2019). For this, a flow cone mould placed on a flow table was filled with fresh mortar. Then, the mould was removed, and 15 vertical shakes were applied at constant speed. The final average diameter determined the value of the consistency of the mortars.

2.5. Hardened state properties of mortars

The hardened state properties studied in the mortars were compressive strength and leaching behaviour, according to XP X31–212:2011 (AENOR, 2019) and XP X31–211:2012 (AENOR, 2019).

The English Environmental Agency (EEA) (EEA, 2010) establishes a minimum compressive strength (1 MPa) of mortars to be considered as monoliths to be able to handle transport, deposit and reduce riskiness. The compressive strength results of 3 specimens of mortars were compared with the EEA acceptance requirement.

Table 2
Nomenclature, dosage, water/cement ratio and water/solid ratio.

Mortars	C (g)	NS (g)	SF (g)	HT (g)	Pb* (g)	Total mass (g)	%W+	w/c	w/s
M0	1200	603	1200	–	–	3003	28.00	0.70	0.282
M15	1200	603	1200	15	–	3018	27.80	0.70	0.278
M30	1200	603	1200	30	–	3033	27.70	0.70	0.277
M60	1200	603	1200	60	–	3063	27.40	0.70	0.274
M120	1200	603	1200	120	–	3123	26.90	0.70	0.267
MPb	1200	603	1187	–	13	3003	28.00	0.70	0.282
MPbN	1200	603	1181	–	19	3003	28.00	0.70	0.282
M120Pb	1200	603	1187	120	13	3123	26.90	0.70	0.267
M120PbN	1200	603	1181	120	19	3123	26.90	0.70	0.267

* This element will be added as PbO and Pb $(NO_3)_2$ to the mixes and denoted as symbol Pb and PbN, respectively.
+ Percentage of water in total mix mass.

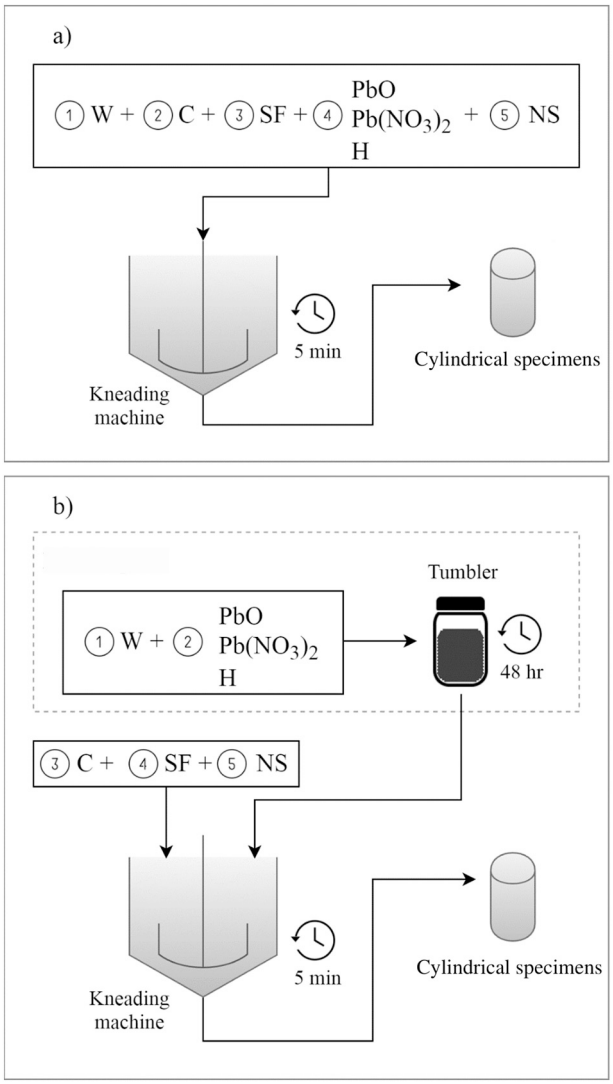

Fig. 4. a) Mixing procedure, A (MProc-A), b) Mixing procedure B (MProc-B).

Additionally, the mineralogical phase formation was analysed in the mortars by XRD. After 28 days, a portion from each mortar was dried at 60 °C during 24 h. Then it was crushed and sieved through a 0.125 mm sieve.

In order to study lead mobility, the leaching behaviour of mortars (M0, MPb, MPbN, M120Pb and M120PbN) in monolithic state was evaluated according to XP X31–211: 2012 (AENOR, 2019). This standard provides knowledge of element mobility during the first contact of the material with the leaching liquid (Cyr et al., 2007; Cyr et al., 2012; Ledesma et al., 2017; Ledesma et al., 2018; Quina et al., 2014). Mortars were fully immersed into a polypropylene tank with deionised water as a reagent using a liquid/solid ratio (L/S) of 10 L/kg ± 0.2 L/kg. The samples remained immersed in reagent for 24 h at a temperature of 20 °C ± 5 °C and were moved through a magnetic agitator at 120 rpm ± 20 rpm. After the test time, an eluate was filtered with a 0.45 μm filter and analysed with a Perkin Elmer ELAN DRC-e mass spectrometry (ICP-MS). This procedure was repeated 2 times for each mortar.

The EU Council Decision (2003) on waste acceptance in landfills establishes the "Inert", "Non-hazardous" and "Hazardous" limits for granular materials according to the levels of heavy metal release in leachates. If leachate concentrations exceed the "Non-Hazardous" limit, for only one element, the materials are considered "Hazardous". Legislation on the limits of monolithic materials is still non-existent (Castro and García, 2010). In the absence of monolithic limits, the EEA (2010) proposed that the results obtained through the monolithic leaching test be compared with the limits established in the EU Council Decision (2003). In this study, the limits used corresponded to the lead element (Table 3).

3. Results and discussion

3.1. Lead adsorption isotherm

First, the interaction between lead and HT was addressed, due to its possible influence on the setting of cementitious matrices that incorporate hydrotalcite. The lead adsorption isotherm in HT is shown in Fig. 5, where C_e (mg/L) is the equilibrium concentration of metal ion in the solution and C_s (mg/kg) is the amount of ion adsorbed (lead) per weight unit of adsorbent (HT) after equilibrium. The Freundlich isotherm model was used to fit the experimental data of the adsorption isotherm. The dotted line in Fig. 5 represented the model of the Freundlich equation, which can be represented in logarithmic form by the eq. (1):

$$log\ C_s = log\ k_F + \frac{1}{n_f} log\ C_e \quad (1)$$

where k_F and n_f are factors representing the capacity and affinity adsorption.

It was observed that C_s increased with the rise in C_e, indicating that as the medium concentration increased the lead adsorbed amount by HT rose, reaching values close to 80 mg/kg. The Freundlich model fitting represents adsorption results on heterogeneous surfaces (Tan et al., 2007), meaning the total surface does not show an identical adsorption and, therefore, the lead ions compete and interact with each other. The adsorbent surface was not very heterogeneous because the value of $1/n_f$ did not get closer to zero (Haghseresht and Lu, 1998); in this study it was 0.72. The adsorption is favourable because $n_f > 1$. The larger the n_f value is, the more favourable the adsorption is. In this study n_f was 1.39. From the R^2 values shown in Fig. 5, the experimental data correctly fit the Freundlich isotherm model.

3.2. Fresh state properties of mortars

3.2.1. Heat of hydration

Fig. 6 shows the heat flow released and normalised by sample mass (W/g) as a function of time (min) during the hydration of the mortars. In Fig. 6a and b it was observed that the highest heat flow for M0 was around 380 min. The heat flow of the mortars with HT was similar in time, with all the mortars registering the induction period between 380 and 480 min in MProc-A (Fig. 6a) and between 380 min and 400 min in MProc-B (Fig. 6b). It was noted that the HT presence slightly delayed the mortar hydration, the greater their content in the mixes, as indicated in the displacement towards longer times of the corresponding heat release peak with the Alite hydration (C_3S) (Xie and Biernacki, 2011). The heat release peak corresponding to dissolution of C_3A with formation of Ettringite was also slightly modified by the incorporation of HT. The incorporation of HT led to a shoulder in the heat flow, between 600 min and 800 min in the MProc-A (Fig. 6a) and between 450 min and 900 min in the MProc-B (Fig. 6b), indicating the formation of secondary Ettringite (Bullard et al., 2011; Scrivener et al., 2015). This effect did not appear in M0. Regarding the heat flow released, the changes were not dramatic, reaching values of around 0.0015 W/g and 0.0018 W/g for mortars with the HT addition in both mixing procedures. The differences

Table 3
Legal limits of EU Council Decision 2003/33/EC (2003) (L/S = 10 L/Kg) for Pb.

	Inert	Non-Hazardous	Hazardous
Pb (mg/kg dry matter)	0.50	10.00	50.00

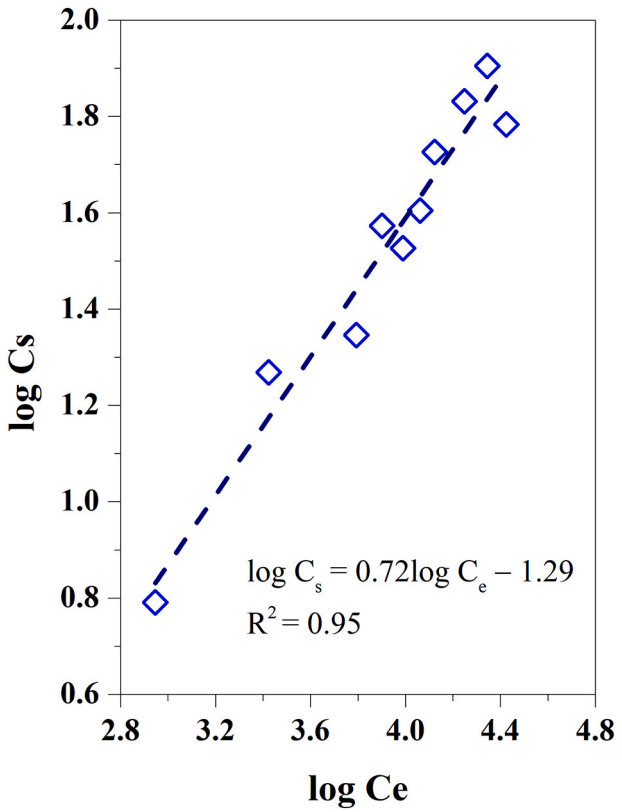

Fig. 5. Adsorption isotherm and Freundlich model fitting for interaction between lead and hydrotalcite. Symbols denote experimental results and solid line represent the linear model of Freundlich equation.

in heat released found by the authors Wu et al. (2018) were also minimal. These authors added hydrotalcite with carbonate calcined in percentages of 1, 2 and 3% regarding the total mass of cement paste. In the current study the amount of hydrotalcite used was between 0.5 and 3.84% regarding the total mass of cement paste. They observed an evolution in the heat of hydration very similar to the control mortar with the same induction period. In the research carried out by Cao et al. (2018) it was observed that the cement slurries with 0.025% Ca-Al-LDH had a negligible effect on the hydration rate. However, when the Ca-Al-LDH dosage was 0.10%, the main hydration peak shifted to earlier times, slightly increasing the amount of heat released. The carbonate-containing hydrotalcite hindered the formation of nucleation points for the precipitation of hydration products by decreasing the amount of reactive particles in the cement matrix (Moon et al., 2017; Thongsanitgarn et al., 2014), which would explain the light delay in releasing heat of hydration.

Fig. 6c and d show a shift in time of heat release compared to M0, when lead was incorporated, in any of its forms, and combined with HT, corresponding to the maximum hydration of C_3S. This displacement indicated a delay in the mortar hydration. For MProc-A, the induction period shifted from 380 min (M0) to approximately 1170 min for MPb and MPbN (Fig. 6c). In MProc-B (Fig. 6d) the values reached approximately 550 min in MPb and 1400 in MPbN. The delay in the mortars with lead content was in accordance with the research of other authors (Nestle, 2004; Weeks et al., 2008).

When HT was added to the mortars with lead content, the time displacement of the heat flow was higher, reaching 1770 min and 1600 min for M120Pb and M120PbN, in MProc-A (Fig. 6c) and 1400 min and 1450 min for M120Pb and M120PbN, in MProc-B (Fig. 6d). In all the cases in which lead was incorporated into the mortars, there was a prolongation of the induction period and a clear deceleration of the C_3S hydration process. Lead hydroxides are expected to precipitate in the alkaline environment of cement hydration (Thomas et al., 1981). Since lead ions are amphoteric, hydroxide precipitates would re-dissolve in the presence of excess hydroxide ions to form plumbite species (PbO_2^{2-}) that clear delaying the setting period (Lasheras-Zubiate et al., 2012; Cocke, 1990; Weeks et al., 2008). Additionally, it is important to highlight that for the samples with lead and without hydrotalcite, the mixing procedure considerably affected the induction period (Duran et al., 2016).

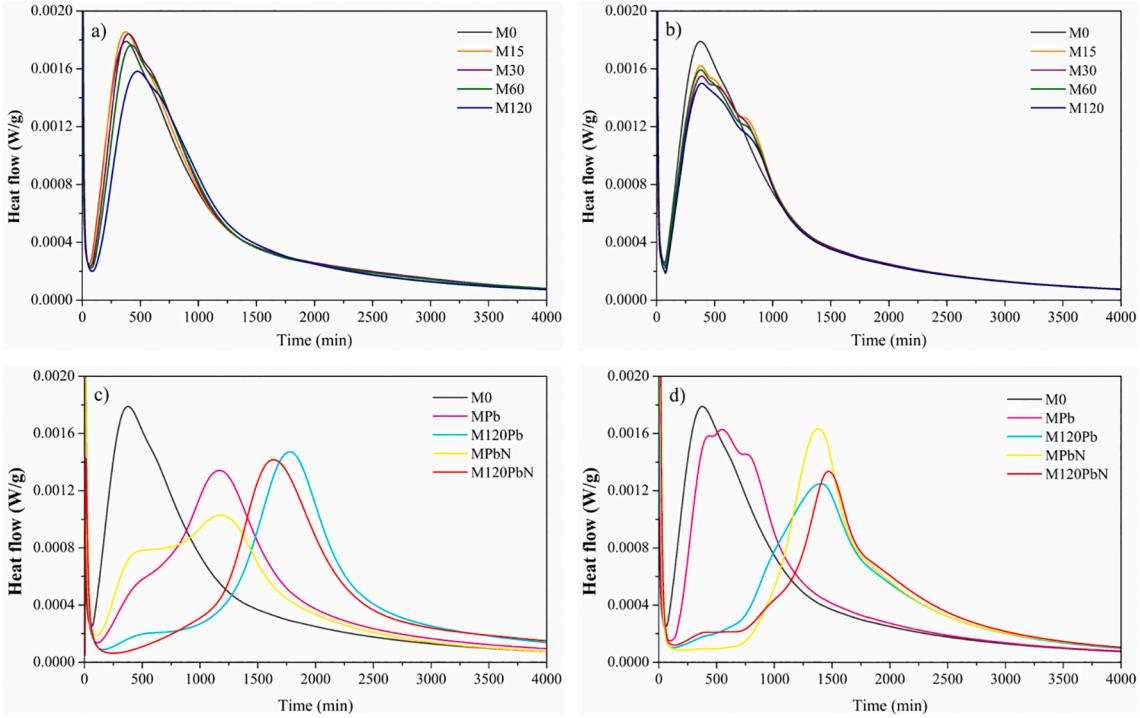

Fig. 6. Heat flow values: a) and c) MProc-A; b) and d) MProc-B.

Fig. 7 represents the surface interaction between HT and plumbite formed in the alkaline environment of cement hydration.

Fig. 8 shows the cumulative heat flow values of the mortars. In Fig. 8a and b it was observed that the evolution of the cumulative heat flow was very similar in all the mortars with HT, reaching values between 100 J/g and 110 J/g, M120 being the lowest cumulative heat flow value. The cumulative heat flow value during mortar hydration was in accordance with their experienced heat flow (Fig. 6a and b. Fig. 8c and d showed the delay undergone by the mortars MPb, MPbN, M120Pb and M120PbN (Fig. 6c and d), especially when HT was added. However, the cumulative heat flow of all the mortars was very similar to M0, registering values between 100 J/g and 112 J/g after 4000 min. The different mixing procedure, in terms of total heat released, did not register significant changes. The delay effect was mostly related to a kinetical effect at early hydration times and after 4000 min all mortars reached similar values to M0. The mixing procedure influenced the form of the curve in cumulative heat flow (Fig. 8c and d depending on lead waste used (solid or liquid). However, when HT is incorporated it does not affect the form of the curve in terms of cumulative heat flow. HT incorporation homogenised these results.

3.2.2. Workability

The workability results (min) of mortars with MProc-A and MProc-B are shown in Fig. 9. Workability results correspond to the average of 3 measurements. The mortars exhibited greater workability as HT content increased, reaching a maximum value of 216 min for the M120 mortar with MProc-A. A similar behaviour was observed in the mortars mixed with MProc-B. This is in accordance with a slight delay in the heat flow of hydration as the hydrotalcite content increased (Fig. 6 a and b) giving rise to a delay in setting time. However, this last mixing procedure affects, to a lesser extent, the workability time compared to M0, increasing up to 166 min for the M120 mortar. Despite the greater amount of material in the mixes with addition of HT, the small delay in the workability time was probably fostered by the formation of a protective hydrotalcite coat over the cement grains, hindering the contact between mixing water and the cement (Cao et al., 2018). The changes in the workability time of mortars with HT content, especially in the second procedure, were not significant compared to the reference mortar; the use of HT in cementitious materials was assumed to be compatible.

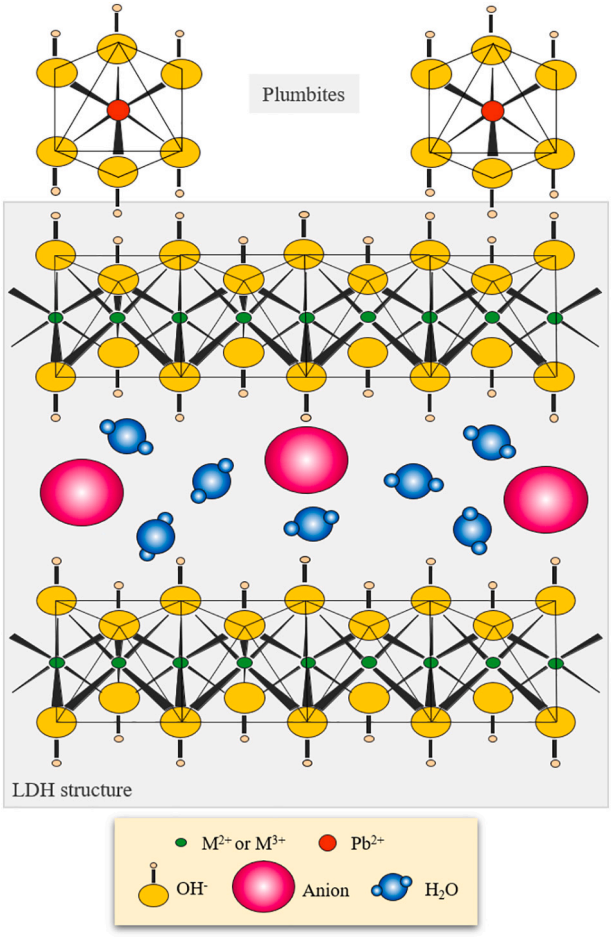

Fig. 7. Surface interaction between hydrotalcite and plumbite.

There was a large increase in the workability time of mortars with lead content in any of its forms. Using MProc-A the workability values increased from 114 min for M0 up to 376 min and 342 min for MPb and MPbN. The values for mortars in MProc-B also increased up to 255 min and 240 min for MPb and MPbN. This is in accordance with a slight delay in the heat flow of hydration as the hydrotalcite content increased (Fig. 6 c and d). An increase in workability time was also observed by Lasheras-Zubiate et al. (2012) when the $Pb(NO_3)_2$ was incorporated to mortars produced with CEMII-32.5 N cement and a load of 1% by weight heavy metal/cement, in the current paper was 0.98%. Since the solubility of these compounds is very low, these authors reported that a small amount of them (approximately 0.15% by weight of the lead mix) could produce significant effects in the delay of cement hydration. This fact was in accordance with the results in the current research because the weight of lead was between 0.27 and 0.39%. In the second procedure the effect was less pronounced.

The workability time was significantly modified with the addition of HT. The simultaneous effect hydrotalcite and lead increased the delay much more markedly than the one due to the sum of the effects separately. The MPb and MPbN mortars increased workability time from 376 min and 342 min up to 1530 min and 1495 min in the MProc-A and from 255 min and 240 min up to 1509 min and 1765 min in the MProc-B. The combined effect of the partial dissolution of lead (plumbites formation) (Lasheras-Zubiate et al., 2012) and the partial coating of cement particles with HT (Cao et al., 2018) seemed to be more intense than the effects separately. This behaviour was in accordance with the results recorded in the heat flow of hydration (Fig. 6 c and d).

When HT was added, very similar behaviour was experienced in both mixing procedures. Therefore, the delay in workability time was mainly linked to the mix composition and the interference between their constituents and not to the mixing procedure used. Using HT, the workability results were homogenised regarding the heat flow and cumulative heat flow (Figs. 6 and 8) regardless of the mixing procedure. In the absence of HT there was no direct correlation between workability and heat flow results using the different mixing procedures.

3.2.3. Flow table values

Fig. 10 shows the flow table results in mm of the mortars in MProc-A and MProc-B. These values correspond to the consistency of the mortar as a result of the average of 2 measurements perpendicular to each other on the mortar cake after the test. A decrease in the flow table values of the mortars was observed when the HT content was higher in the mixes. Since HT was added to the mixes, there was a greater amount of solid in the mixes for the same quantity of available water (Table 2). Although the w/c ratio remained constant, the availability of water in the mix decreased with HT as an addition (water/solid ratio decreased in Table 2).

Authors such as Yang et al. (2015) also detected a decrease in the flow table values of the mortars when they studied the replacement of cement by two hydrotalcites modified with p-aminobenzoate and sodium nitrite. In this research, the decrease in flow table values was very similar in MProc-A and MProc-B. The flow table ranged from 206 mm for M0 to 165 and 160 mm for M120 in MProc-A and MProc-B. The standard UNE EN-1015-3:2000 (AENOR, 2019) does not specify any lower or upper limit value of optimum flow table of fresh mortar, therefore the flow table value will be established according to the mortar use in each

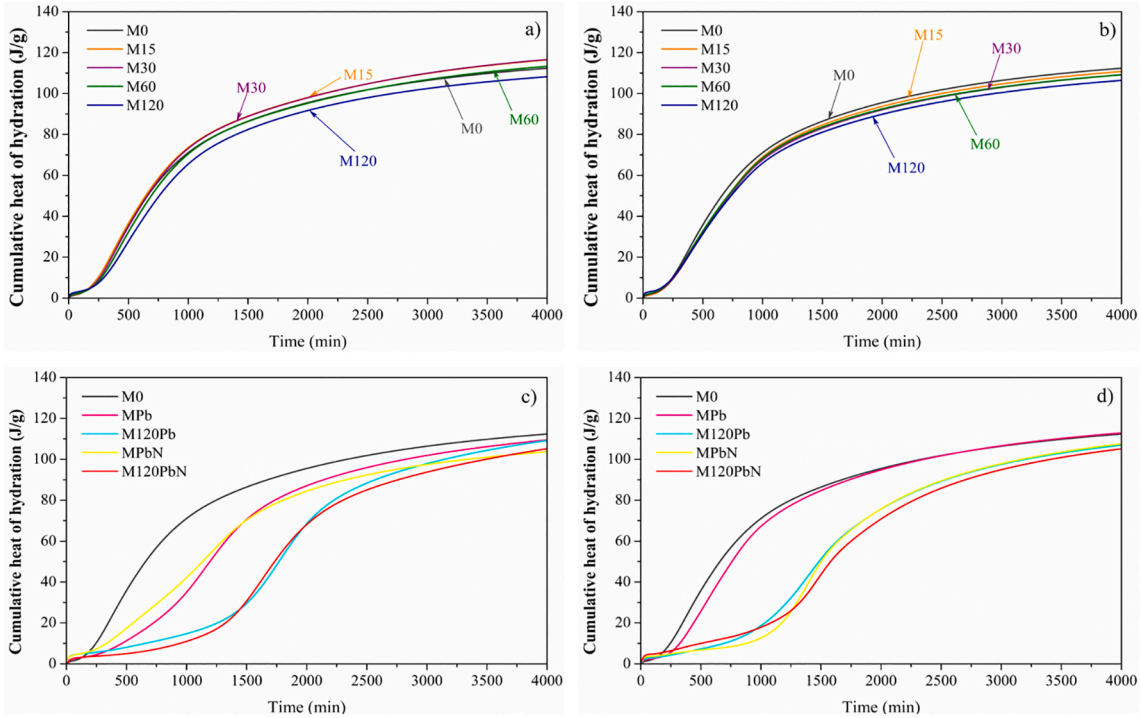

Fig. 8. Cumulative heat flow values: a) and c) MProc-A; b) and d) MProc-B.

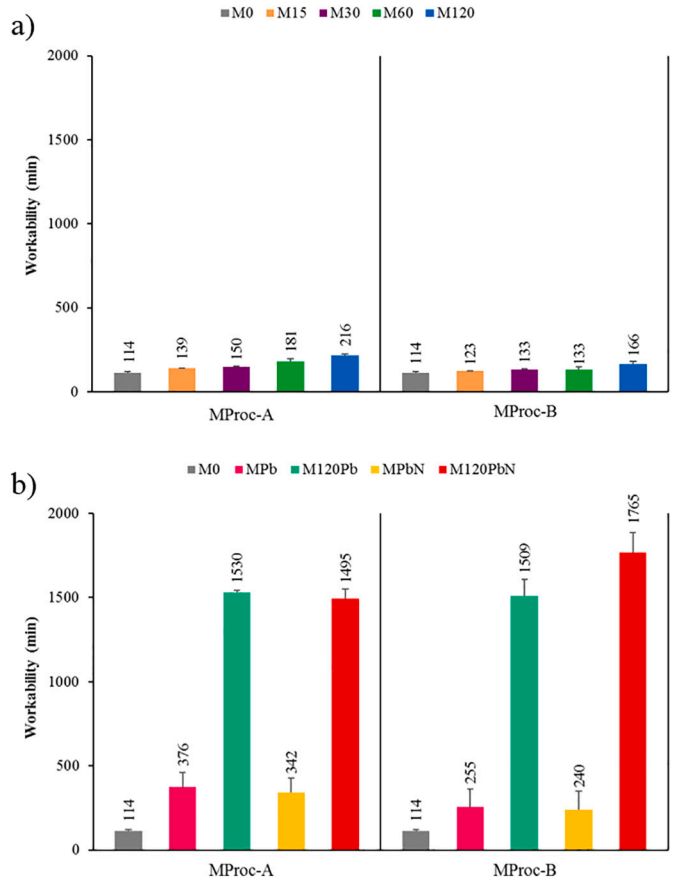

Fig. 9. Workability: a) Mortars with HT (MProc-A and MProc-B; b) Mortars with lead and with lead and HT (MProc-A and MProc-B).

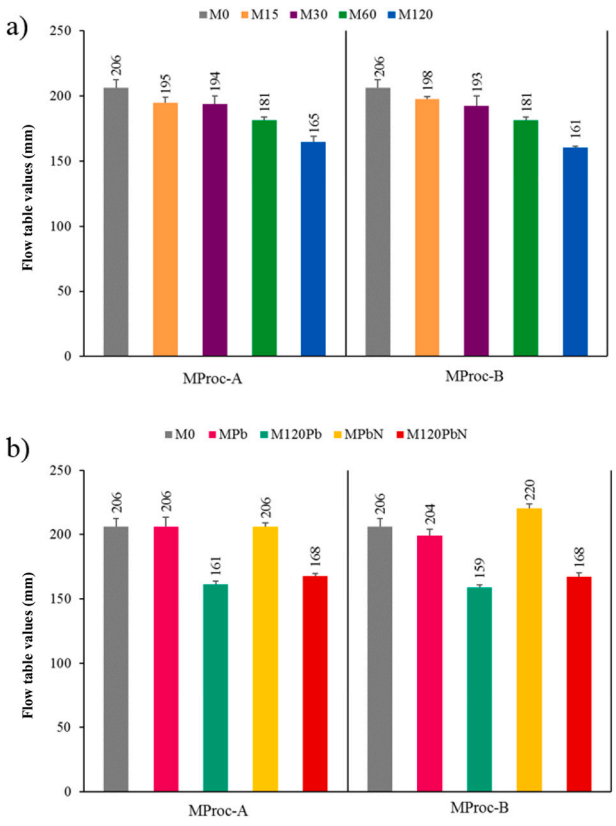

Fig. 10. Flow table values: a) Mortars with HT (MProc-A and MProc-B); b) Mortars with lead and with lead and HT (MProc-A and MProc-B).

case. Despite the decrease in flow table values compared to M0, the results for both mixing procedures were validated since the mixing and subsequent handling of the mortars were considered as adequate.

Consequently, the mixing procedure did not influence the flow table values registered by mortars with hydrotalcite content in the fresh state, since this property is linked to the w/c ratio. Senff et al. (2009) pointed out that the w/c ratio was the most relevant variable in the study of flow table of the mixes produced.

MPb in both mixing procedures (206 mm and 204 mm in MProc-A and MProc-B) and MPbN in MProc-A (206 mm), showed flow table values very close to M0, since the mass in the mixes was the same (3003 g, Table 2). The same behaviour was shown by M120Pb (161 mm and 159 mm in MProc-A and MProc-B) and M120PbN (168 mm in MProc-A and MProc-B), which had the same mass as M120 (3123 g, Table 2), showing flow table values in the range of M120 (Fig. 10b).

Different behaviour was found in MPbN (MProc-B). This mortar contained the same total mass as M0 (3003 g, Table 2) and recorded a value of 206 mm in MProc-A. However, the MProc-B increased the flow table values to 220 mm, which meant an increase of 6.7%, and the quantity of $Pb(NO_3)_2$ was 1.6% in weight compared to cement. Lasheras-Zubiate et al. (2012; 2011) also experienced an increase in the flow table values of 3% when they incorporated 1%, by weight compared to cement, of $Pb(NO_3)_2$ dissolved in the mixing water of mortars. It can be concluded that the presence of lead does not practically affect the flow table values, nor the mixing procedure, except in the case of the MPbN sample already mentioned.

3.3. Hardened state properties of mortars

3.3.1. Compressive strength

The results of compressive strength when HT is incorporated into the mortars at 28 days are shown in Fig. 11a. The M0 showed a compressive strength value of 34.64 MPa. A decrease tendency of compressive strength was observed with the HT incorporation in the mortars with values of 34.92 MPa, 32.15 MPa, 30.41 MPa and 29.90 MPa for M15, M30, M60 and M120 in MProc-A, and values of 30.37 MPa, 30.77 MPa, 29.29 MPa and 28.86 MPa for M15, M30, M60 and M120 in MProc-B. The maximum decrease was 16.69%. As for the results of mortar compressive strength after 28 days, the influence of the mixing procedure was negligible.

The compressive strength loss had also been observed by authors such as Yang et al. (2015) and Cao et al. (2018). In the research carried out by Yang et al. (2015) compressive strength decreased by 17.20% compared to the control mortar at 28 days due to the replacement of 10% of the cement by a hydrotalcite modified with p-aminobenzoate. In the study by Cao et al. (2018) the decrease in compressive strength at 28 days was 18.95% in cementitious slurries with 0.4% Ca-Al-LDH replacement of cement weight. These authors attributed compressive strength loss to the formation of a protective coat on the cement particles that decreased and delayed the hydration reaction rate of the cement. The slightly larger decrease in the second mixing procedure could be attributed to the greater and better HT dispersion over the particles by increasing their dispersion in the mixing water prior to mixing this with the dry components.

The compressive strength loss recorded by other authors had a similar magnitude to that of this research, this maximum decrease being approximately 17.20% (Yang et al., 2015) and 18.95% (Cao et al., 2018). The compressive strength results of the mortars with the HT addition were in accordance with the heat flow values (Fig. 6) and cumulative heat flow values (Fig. 8) of the mortars during their hydration.

The influence in compressive strength of the presence of lead or simultaneously lead plus HT was observed. With the objective to analyse the maximum effect the mix with higher amount of HT was selected. The MProc-A mixing procedure (Fig. 11b) affected the compressive strength values to a greater extent, decreasing them from 34.64 MPa for M0 to 26.77 MPa and 27.31 MPa for MPb and MPbN. The compressive strengths of MPb and MPbN in the MProc-B were equal to 30.40 MPa and 33.19 MPa, indicating that the mixing method used was important. Navarro-Blasco et al. (2013) observed a compressive strength detriment

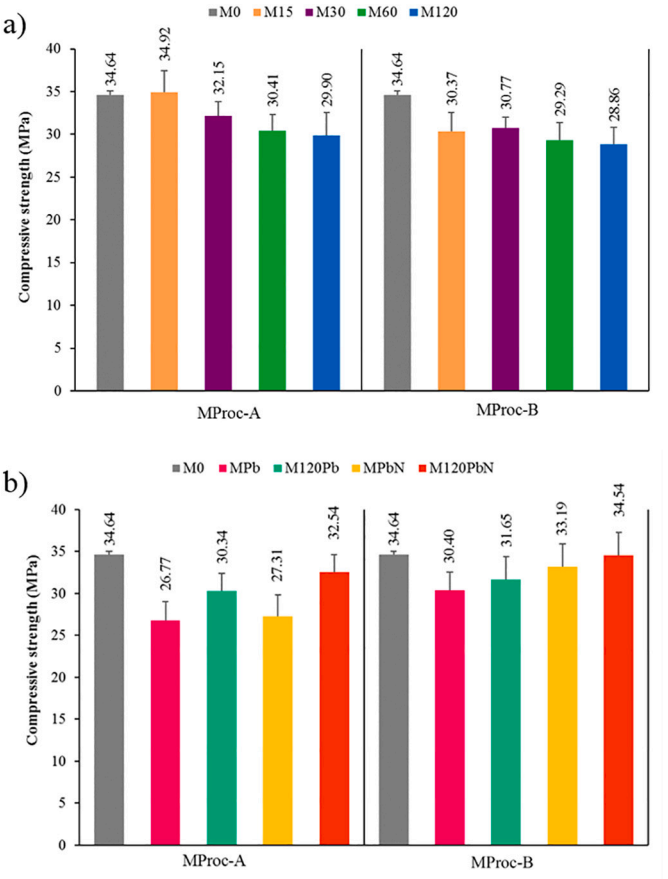

Fig. 11. Compressive strength at 28 days: a) Mortars with HT (MProc-A and MProc-B); b) Mortars with lead and with lead and HT (MProc-A and MProc-B).

of around 75% in mortars doped with 1% $Pb(NO_3)_2$ weight/calcium aluminate cement (CAC). Although these matrices are more suitable for the amphoteric metal encapsulation due to their having low pH, in this study these matrices did not favour the compressive strength values. In the current study the decrease was 21.16% in the first mixing procedure and 4.19% in the second procedure. A compressive strength loss around 65.00% was also detected by Gollmann et al. (2010) when they replaced ordinary Portland cement (OPC) with 10% PbO_2 by weight. In the current paper the loss was 22.72% for the first procedure and for the second around 12.24% was observed.

When the hydrotalcite was incorporated into the mortars in MProc-A, the compressive strength values were beneficial compared to mortars without hydrotalcite. That is, MPb and MPbN increased their compressive strength value from 26.77 MPa and 27.31 MPa to 30.34 MPa and 32.54 MPa for M120Pb and M120PbN. The greater amount of material in the matrix with the HT addition could counteract the effect exerted by the lead in the compressive strength loss. In MProc-B all compressive strength values increased with the HT incorporation into the mortars, since there was a greater and better dispersion of the adsorbent and the metal, and the combined effect was less, having a lower consequence on this property. In short, when HT is used, the effect of the mixing procedure was negligible on the compressive strength of the mortars. All the compressive strength results experienced in the mortars when HT was used and in MProc-B were in accordance with the cumulative heat of release; that is, the heat gain trend was very similar after 4000 min (100–110 J/g), and therefore the performance of compressive strength over time obtained very close values (30.40 MPa – 34.64 MPa) for all these mortars.

3.3.2. Mineralogical phases study

Figs. 12-15 show the mineralogical phases formed in the mortars after 28 days. In all mortars characteristic phases of cement hydration and of the aggregates were registered, such as Portlandite ($Ca(OH)_2$; 04–0733), Quartz (SiO_2; 33–1161), Calcite ($CaCO_3$; 05–0586), Ettringite ($Ca_6Al_2(SO_4)_3(OH)_{12}{\cdot}26H_2O$; 41–1451), dicalcium silicate (C_2S; 24–0034), tricalcium silicate (C_3S; 42–0551) Gypsum ($CaSO_4{\cdot}2H_2O$; 33–0311) and hydrotalcite ($Mg_6Al_2(CO_3)(OH)_{16}{\cdot}4H_2O$; 14–0191) were also observed in some mortars (JCPD, 1995). Additionally, Orthoclase ($K(AlSi_3O_8$; 86–0438) was detected in MPb using MProc-B mixing procedure (Fig. 15). No noticeable differences were observed in the crystallinity of the different phases during setting when HT and lead were part of the composition.

In the MPb and MPbN mixed by MProc-B (Fig. 15) reflections located between 27.3° and 28.3° (2θ) were detected. These phases were not registered in the reference mortar (M0). Lead Oxide (PbO; 35–1482) attributable to the reflection recorded in MPb and Lead Nitrate Hydroxide ($Pb(NO_3)OH/Pb(NO_3)_2{\cdot}Pb(OH)_2$; 22–0388) (JCPD, 1995) corresponding to the peak recorded in MPbN were detected. The greater and better dispersion of the metal in MProc-B allowed a medium more favourable to the lead compound formation. Due to the lead low load compared to the rest of the mortar components and the mainly siliceous composition of the samples, the lead phase identification by XRD was masked by the most crystalline and majority phases. It should be noted that the phases Lead Oxide (PbO; 35–1482) and Lead Nitrate Hydroxide ($Pb(NO_3)OH/Pb(NO_3)_2{\cdot}Pb(OH)_2$; 22–0388) were not detected in M120Pb and M120PbN, probably due to the lead adsorption on the HT surface not being registerable by XRD.

3.3.3. Leaching behaviour of mortars in monolithic state

Table 4 shows the lead release results in the mortars according to XP X31–211: 2012 (AFNOR, 2019), as well as the parameters of pH, temperature and conductivity, measured during the test. Included next to the lead leaching value is the environmental classification according to

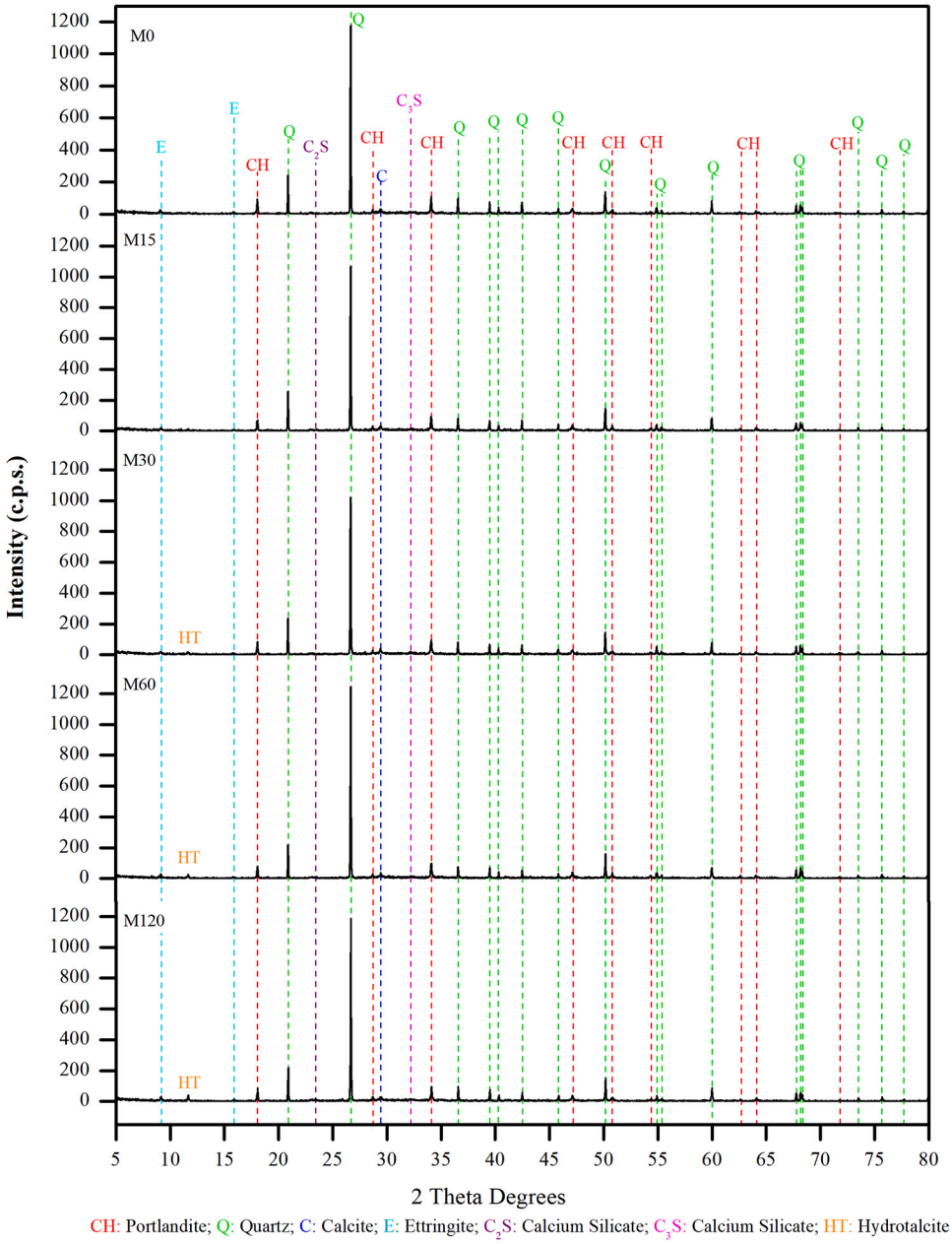

Fig. 12. XRD patterns of MProc-A mortars with HT.

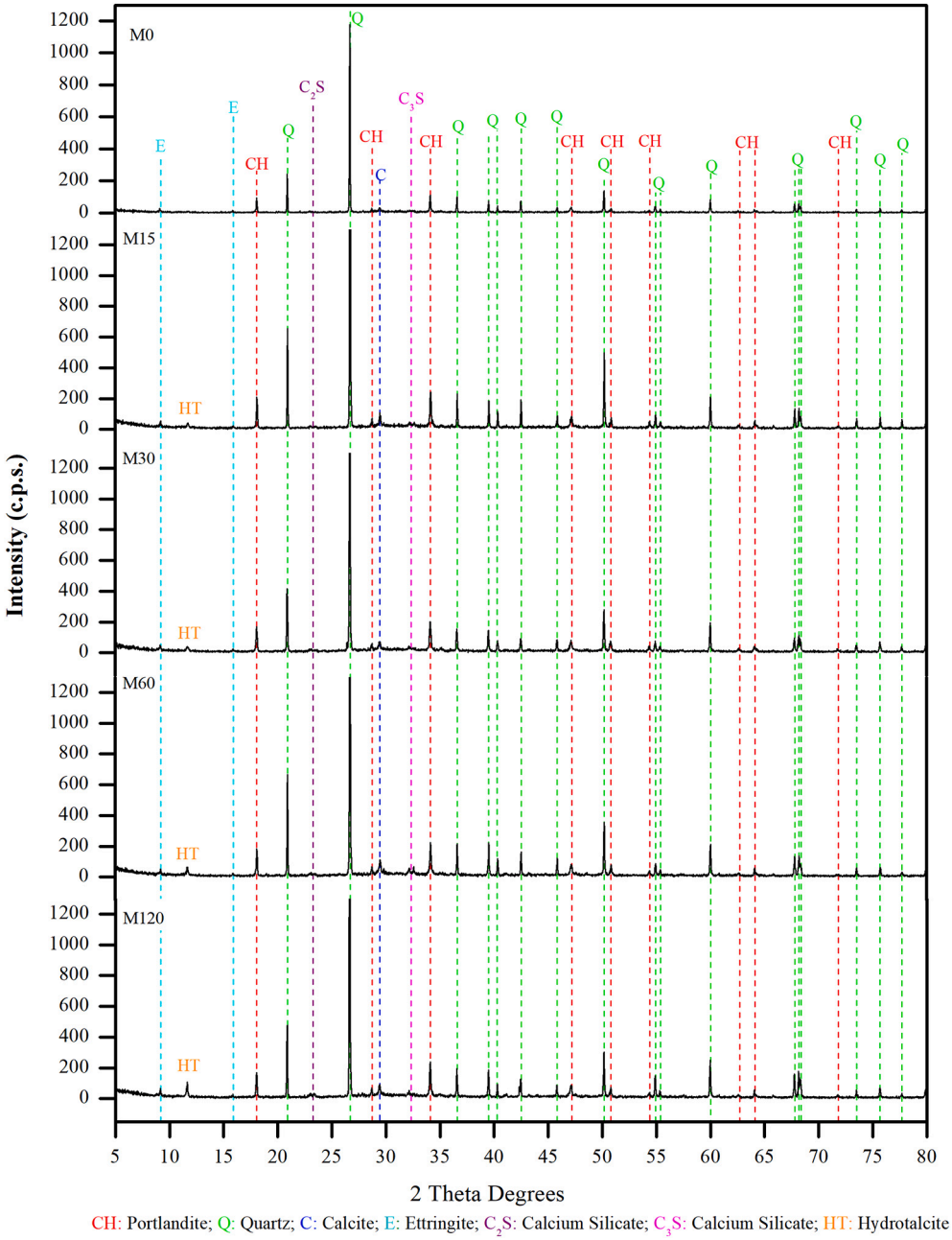

Fig. 13. XRD patterns of MProc-B mortars with HT.

the limits established in the EU Council Decision (2003).

M0 obtained an "Inert" environmental classification. The rest of the mortars kept the lead release below the limit of 10.00 mg/kg dry matter; therefore, they complied with the "Non-Hazardous" code.

Regarding the different mixing procedures, all mortars registered a lower lead leaching in the MProc-A. MPb achieved a lead release equal to 0.71 mg/kg in the MProc-A, while this was 1.52 mg/kg in the MProc-B. The lead release in the MPbN was 0.85 mg/kg and 1.10 mg/kg in MProc-A and MProc-B.

Mortars with HT content also recorded less lead leaching mixed by MProc-A, with values of 0.52 mg/kg for M120Pb and 0.73 mg/kg for M120PbN, compared to 0.72 mg/kg and 0.86 mg/kg recorded in MProc-B. This phenomenon was related to the fact that the lead content was previously kept in the mixing water increasing the dissolution of lead and therefore its release potential was higher in MProc-B. In summary, the incorporation of HT homogenised the lead leaching results.

The HT incorporation to the mortars reduced the leaching of the monolithic samples mixed by MProc-A. M120Pb and M120PbN decreased the lead release from 0.71 mg/kg and 0.85 mg/kg to 0.52 mg/kg and 0.73 mg/kg. This reduction represented approximately 27% and 14%, respectively. The HT addition in mortars improved the metal immobilisation improving waste management with lead content in solid state from a leaching behaviour point of view. The lead release was also reduced by the incorporation of HT in MProc-B. In MPb the release from 1.52 mg/kg to 0.72 mg/kg (M120Pb) was reduced, assuming a reduction rate of approximately 53%. For $Pb(NO_3)_2$ leaching decreased from 1.10 mg/kg for MPbN to 0.86 mg/kg for M120PbN, representing a reduction percentage of 22%. The HT addition in mortars improved the metal immobilisation improving waste management with lead content in aqueous state from a leaching behaviour point of view.

These commented results confirming the efficacy of HT applied in this study are partly due to the surface interaction between lead and HT

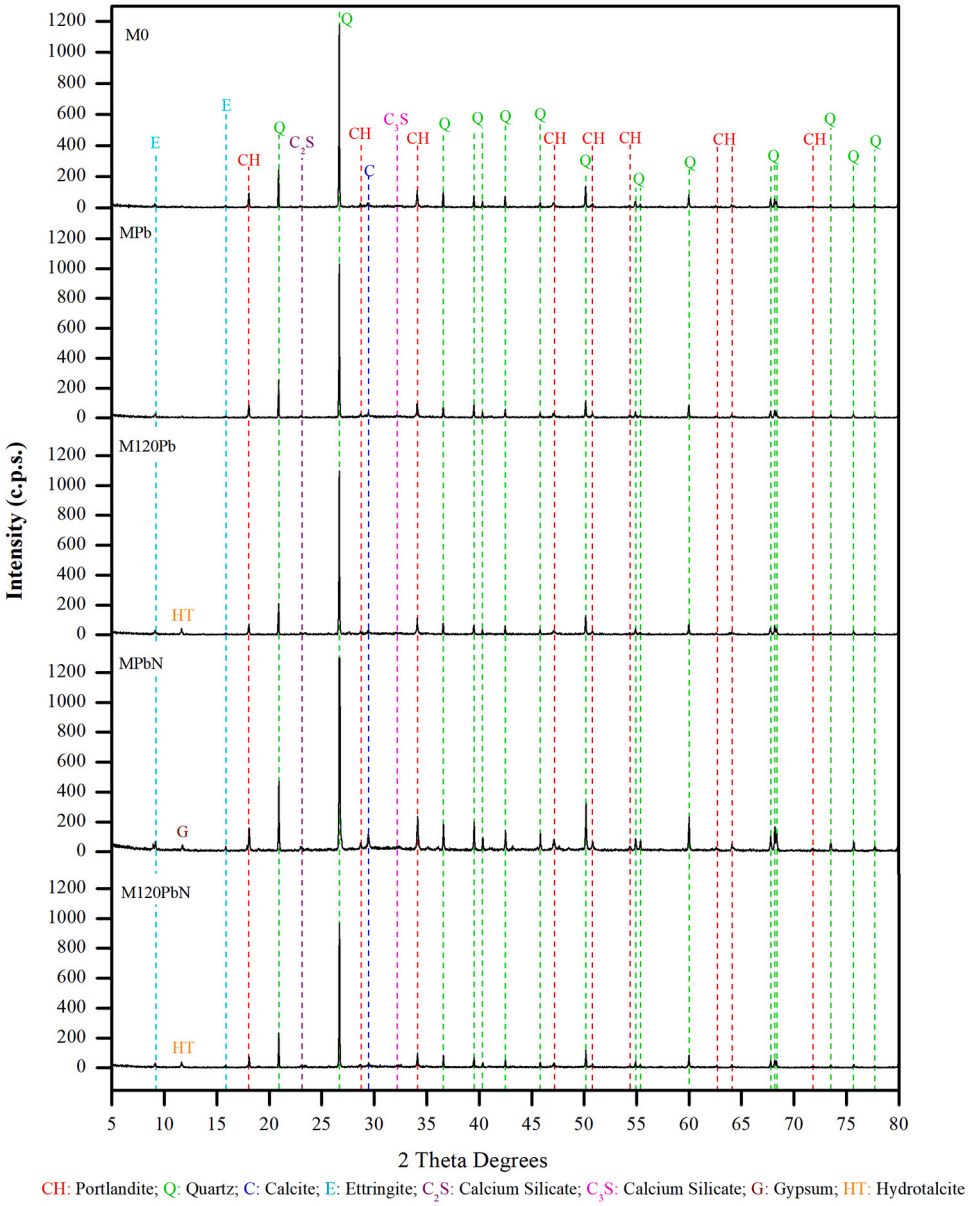

Fig. 14. XRD patterns of MProc-A mortars with lead and with lead and HT.

already commented (Fig. 7).

In short, when the cementitious matrices include a Mg—Al hydrotalcite the lead leaching in both mixing procedures decreases to values include in "Non-Hazardous" code (<10.00 mg/kg dry matter) very close to "Inert" code (<0.50 mg/kg dry matter).

4. Short discussion

The hydrotalcite presence slightly delayed the mortar hydration. The induction period was slightly delayed with the hydrotalcite increase in mortars, indicated by the displacement towards longer times of heat peak related to the Alite (C_3S), probably due to the greater presence of non-reactive particles. However, in terms of total heat release, the results were very similar. This delay was in accordance with the recorded data of workability time, where the increase could be related to the formation of a hydrotalcite protective coat on cement particles. The lower water availability in the mixes caused a slight decrease in the flow table values because of the addition of hydrotalcite.

Authors such as Navarro-Blasco et al. (2015) reported a similar behaviour in consistency and workability time properties in stabilisation mortars of phosphate coating sludge. As the sludge/cement ratio increased, the consistency decreased while the workability time increased as a result of the heavy metals in the sludge.

The small changes in the hydration of the mortars with hydrotalcite content had a slight effect on the compressive strengths, decreasing them with the increase in the hydrotalcite content. However, the maximum compressive strength loss represented 16.69%, all mortars registered strengths above 28 MPa, confirming compatibility between the hydrotalcite and the mortar. This compatibility was also demonstrated in the formation of the same mineral phases (XRD) in all mortars with hydrotalcite content. In short, the changes in mortars when hydrotalcite was added were not dramatic, therefore, the compatibility between the hydrotalcite and the cementitious matrices was verified.

The lead incorporation delayed the induction period of the mortars. This delay increased to a greater extent with the incorporation of hydrotalcite; however, the cumulative heat flow released was very close for all mortars, so the delay effect happened in the early hydration times. When hydrotalcite was part of the mortars, the results of heat flow and

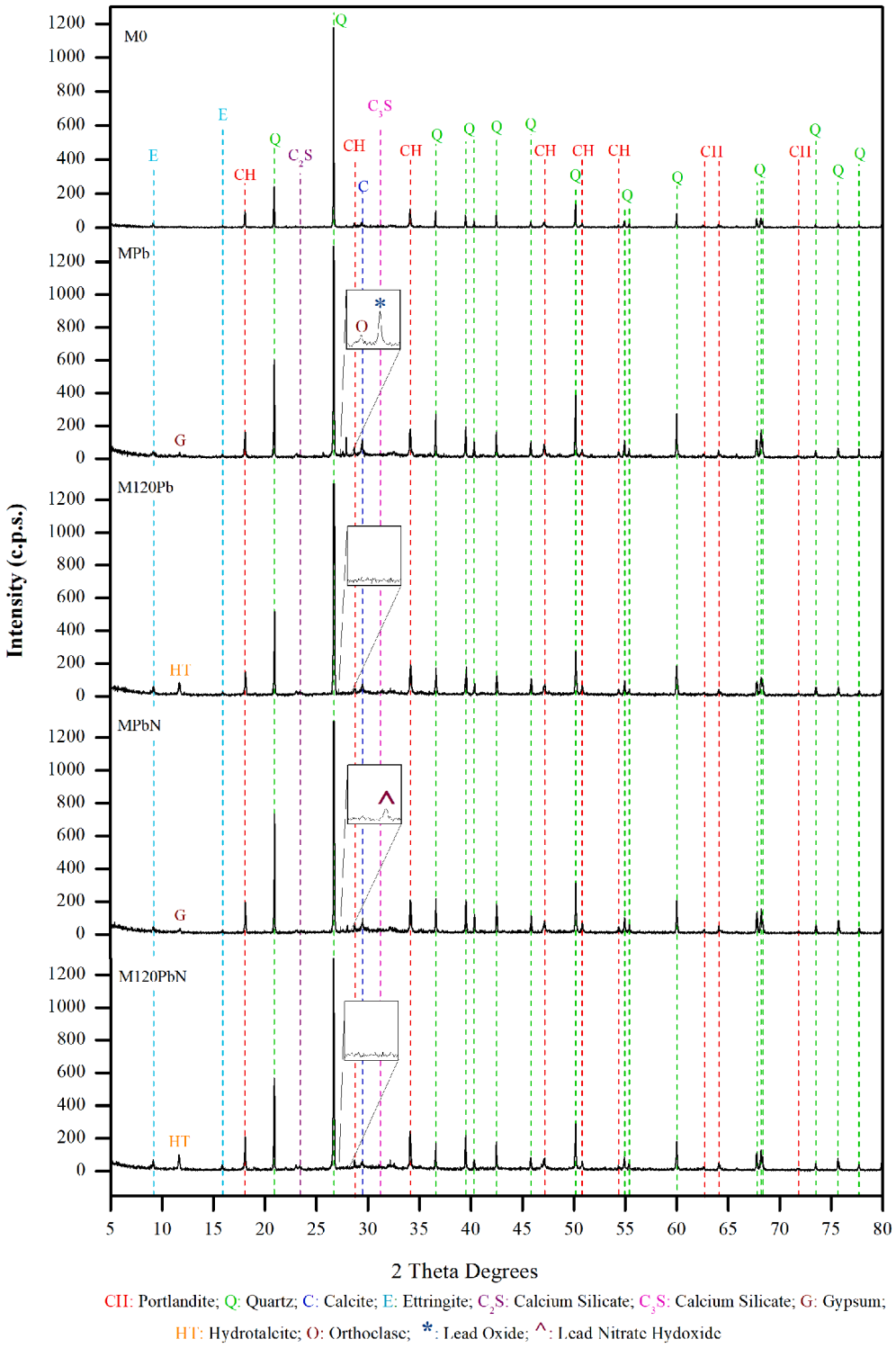

Fig. 15. XRD patterns of MProc-B mortars with lead and with lead and HT.

cumulative heat flow were related to the workability behaviour experienced regardless of the mixing procedure. The addition of the hydrotalcite homogenised the results. Additionally, the flow table behaviour was linked to the material amount in the mix. By maintaining a constant water/cement ratio in the investigation, mortars with the same total mass recorded very similar flow table results.

The compressive strengths of the mortars were maintained above 26 MPa. The compressive strength was increased with the hydrotalcite incorporation to the mortars with lead in both mixing procedures. The compressive strength of all mortars with hydrotalcite and in the mixing procedure B, agreed with the similar heat gain trend. In all mortars the characteristic phases (XRD) of cement hydration were registered. In mortars without hydrotalcite in mixing procedure B there appeared minority phases related to lead. These lead phases were not detected in homonymous mortars with hydrotalcite.

The hydrotalcite incorporation to the mortars reduced the lead leaching of the monolithic samples in both mixing procedures, partly due to the surface interaction between the hydrotalcite and lead (Fig. 7).

Table 4
Release levels of Pb according to XP X31–211 (AFNOR, 2019) after 28 days.

[A] Parameters in studied samples	MProc-A	MProc-B
M0		
pH	11.56	–
Conductivity	1070	–
Temperature	21.10	–
Pb leaching	0.00[I]	–
MPb		
pH	11.82	11.53
Conductivity	933.50	850.00
Temperature	21.60	26.90
Pb leaching	0.71[NH]	1.52 [NH]
M120Pb		
pH	11.82	11.54
Conductivity	835.25	798.00
Temperature	21.93	27.65
Pb leaching	0.52 [NH]	0.72 [NH]
MPbN		
pH	11.68	11.57
Conductivity	1024.00	846.00
Temperature	25.15	29.00
Pb leaching	0.85 [NH]	1.10 [NH]
M120PbN		
pH	11.77	11.57
Conductivity	784.00	784.50
Temperature	21.35	27.30
Pb leaching	0.73 [NH]	0.86 [NH]

[A] Values at 28th day for Conductivity, Temperature and Pb leaching expressed in μS cm^{-1}, °C and mg/kg dry matter, respectively.
[I] Inert material (< 0.50 mg/kg dry matter); [NH] Non-Hazardous (< 10 mg/kg dry matter) and [H] Hazardous (> 10 mg/kg dry matter) (EU, 2003).

Mixing procedure A decreased leaching results compared to mixing procedure B. Despite this, the lead leaching in both mixing procedures decrease to values (0.52–0.86 mg/kg dry matter) included in the "Non-Hazardous" code of the environmental classification (< 10.00 mg/kg dry matter), very close to "Inert" code (< 0.50 mg/kg dry matter). Therefore, the incorporation of hydrotalcite favoured the control of the mobility of lead waste (solid or liquid), homogenising the leached amounts of lead.

5. Conclusions

This study analysed the influence of Mg-Al-Hydrotalcite in the hydration of cementitious mortars, providing advantages for proper management of waste with lead content in solid or liquid state.

The two main contributions of this research were: firstly, the low interference of the Mg-Al-Hydrotalcite in the properties of mortars in the fresh and hardened state, and secondly, the reduction and homogenisation of leaching results.

Mg-Al-Hydrotalcite slightly modified the cement setting, resulting in longer workability times. These slight changes practically do not influence the compressive strength at 28 days for all mortars. Therefore, the current study verified the compatibility of Mg-Al-Hydrotalcite with cementitious systems.

The simultaneously presence of lead and Mg-Al-Hydrotalcite produced changes in the cement setting and in the workability time. However, the total heat of hydration results reached values close to reference mortar. The addition of Mg-Al-Hydrotalcite improved the compressive strengths of lead mortars in all cases.

Leaching results were especially noteworthy. The use of Mg-Al-Hydrotalcite in cementitious matrices (with solid and liquid lead waste) reduced the lead released and mortars were classified as "Non-Hazardous". The interaction between Mg-Al-Hydrotalcite and lead was possible due to the formation of plumbites in the alkaline environment of cement hydration. The results obtained for mixing procedure B were of special interest because leaching was reduced between 20% and 50% due to the incorporation of Mg-Al-Hydrotalcite.

The properties most strongly affected by the mixing procedure used were compressive strength and leaching. The incorporation of Mg-Al-Hydrotalcite into lead mortars showed the effect of the mixing procedure was negligible. When Mg-Al-Hydrotalcite was not incorporated, the results were different.

In short, this research provides potential sustainable solutions to lead waste management, expanding the type of treated waste by adding a hydrotalcite with low interference with the cementitious matrix.

Declaration of Competing Interest

The authors declare that they have no known competing financial interests or personal relationships that could have appeared to influence the work reported in this paper.

Acknowledgments

This investigation was partially supported by Junta de Andalucía through the Research Groups FQM-391 "Materials and Applications" and TEP-227 "Construction Engineering" and the research project 1262554-R (FEDER 2014-2020). Lozano-Lunar is also grateful for the funding of MECD-Spain (http://www.mecd.gob.es/educacion-mecd/) FPU14/05245. Funding for open access charge: University of Córdoba/CBUA.

References

AENOR, 2019. Asociación Española de normalización y certificación. AENOR, Spain. Available online. www.aenor.es (11 December 2020).
AFNOR, 2019. Association française de normalisation. AFNOR, France. Availabe online. www.afnor.org (11 December 2020).
Asavapisit, S., Naksrichum, S., Harnwajanawong, N., 2005. Strength, leachability and microstructure characteristics of cement-based solidified plating sludge. Cem. Concr. Res. 35 (6), 1042–1049.
Belebchouche, C., Moussaceb, K., Tahakourt, A., Aït-Mokhtar, A., 2015. Parameters controlling the release of hazardous waste (Ni^{2+}, Pb^{2+} and Cr^{3+}) solidified/stabilized by cement-CEM I. Mater. Struct. 48 (7), 2323–2338.
Bullard, J.W., Jennings, H.M., Livingston, R.A., Nonat, A., Scherer, G.W., Schweitzer, J. S., Scrivener, K.L., Thomas, J.J., 2011. Mechanisms of cement hydration. Cem. Concr. Res. 41 (12), 1208–1223.
Cao, L., Guo, J., Tian, J., Xu, Y., Hu, M., Wang, M., Fan, J., 2018. Preparation of Ca/Al-Layered Double Hydroxide and the influence of their structure on early strength of cement. Constr. Build. Mater. 184, 203–214.
Castro, A.M., García, E., 2010. Estudio sobre la aplicación y desarrollo en España de ladecisión 2003/33/CE, del Consejo sobre procedimientos y criterios de admisiónde residuos en vertedero. Available online (May 25, 2021). https://www.miteco.gob.es/images/es/Estudio%20sobre%20la%20aplicaci%C3%B3n%20y%20desarrollo%20en%20Espa%C3%B1a%20de%20la%20decisi%C3%B3n%20200333CE%2C%20del%20consejo_tcm30-192979.pdf.
Chaabane, L., Moussaceb, K., Ait-Mokhtar, A., 2017. Factors affecting the leaching of heavy metals (Ni^{+2}, Pb^{+2}, Cr^{+3}) contained in sludge waste stabilization/solidification by hydraulic benders, part I: water/cement and waste/cement ratio in S/S mortars. Environ. Prog. Sustain. Energy 36 (1), 93–103.
Chen, Q., Hills, C., Tyrer, M., Slipper, I., Shen, H., Brough, A., 2007. Characterisation of products of tricalcium silicate hydration in the presence of heavy metals. J. Hazard. Mater. 147 (3), 817–825.
Chen, Q.Y., Tyrer, M., Hills, C.D., Yang, X.M., Carey, P., 2009. Immobilisation of heavy metal in cement-based solidification/stabilisation: a review. Waste Manag. 29 (1), 390–403.
Cocke, D.L., 1990. The binding chemistry and leaching mechanisms of hazardous substances in cementitious solidification/stabilization systems. J. Hazard. Mater. 24 (2), 231–253.
Cyr, M., Coutand, M., Clastres, P., 2007. Technological and environmental behavior of sewage sludge ash (SSA) in cement-based materials. Cem. Concr. Res. 37 (8), 1278–1289.
Cyr, M., Idir, R., Escadeillas, G., 2012. Use of metakaolin to stabilize sewage sludge ash and municipal solid waste incineration fly ash in cement-based materials. Journal of hazardous Materials 243 (Supplement C), 193–203.
De Angelis, G., Medici, F., Montereali, M.R., Pietrelli, L., 2002. Reuse of residues arising from lead batteries recycle: a feasibility study. Waste Manag. 22 (8), 925–930.
Duran, A., Sirera, R., Perez-Nicolas, M., Navarro-Blasco, I., Fernandez, J.M., Alvarez, J.I., 2016. Study of the early hydration of calcium aluminates in the presence of different metallic salts. Cem. Concr. Res. 81, 1–15.
EEA, 2010. English Environmental Agency. Availabe online. https://www.gov.uk/government/uploads/system/uploads/attachment_data/file/296422/geho1110btew-e-e.pdf (11 December 2020).
EU, 2003. European Council Decision for the acceptance of waste at landfills. Availabe online. https://www.gov.uk/government/uploads/system/uploads/attachment_dat

a/file/296422/geho1110btew-e-e.pdfhttp://eur-lex.europa.eu/LexUriServ/LexUriServ.do?uri=OJ:L:2003:011:0027:0049:EN:PDF (11 December 2020).
Fares, G., Al-Zaid, R.Z., Fauzi, A., Alhozaimy, A.M., Al-Negheimish, A.I., Khan, M.I., 2016. Performance of optimized electric arc furnace dust-based cementitious matrix compared to conventional supplementary cementitious materials. Constr. Build. Mater. 112, 210–221.
Fernández Olmo, I., Chacon, E., Irabien, A., 2001. Influence of lead, zinc, iron (III) and chromium (III) oxides on the setting time and strength development of Portland cement. Cem. Concr. Res. 31 (8), 1213–1219.
Forano, C., Hibino, T., Leroux, F., Taviot-Guého, C., 2006. Chapter 13.1 Layered Double Hydroxides. In: Bergaya, Faïza (Ed.), Developments in Clay Science. Elsevier, pp. 1021–1095.
Fujii, S., Sugie, Y., Kobune, M., Touno, A., Touji, J., 1992. Uptakes of Cu^{2+}, Pb^{2+} and Zn^{2+} on synthetic hydrotalcite in aqueous-solution. Chemical Soc Japan 1-5 Kanda-Surugadai Chiyoda-Ku, Tokyo 101, Japan, pp. 1504–1507.
Gasser, M.S., Mekhamer, H.S., Abdel Rahman, R.O., 2016. Optimization of the utilization of Mg/Fe hydrotalcite like compounds in the removal of Sr(II) from aqueous solution. Journal of Environmental Chemical Engineering 4 (4, part a), 4619–4630.
Gineys, N., Aouad, G., Damidot, D., 2010. Managing trace elements in Portland cement–part I: Interactions between cement paste and heavy metals added during mixing as soluble salts. Cem. Concr. Compos. 32 (8), 563–570.
Gollmann, M.A.C., da Silva, M.M., Masuero, A.B., dos Santos, J.H.Z., 2010. Stabilization and solidification of Pb in cement matrices. J. Hazard. Mater. 179 (1–3), 507–514.
González, M.A., Pavlovic, I., Rojas-Delgado, R., Barriga, C., 2014. Removal of Cu^{2+}, Pb^{2+} and Cd^{2+} by layered double hydroxide-humate hybrid. Sorbate and sorbent comparative studies. Chemical Engineering Journal 254, 605–611.
González, M.A., Pavlovic, I., Barriga, C., 2015. Cu(II), Pb(II) and Cd(II) sorption on different layered double hydroxides. A kinetic and thermodynamic study and competing factors. Chemical Engineering Journal 269, 221–228.
Haghseresht, F., Lu, G.Q., 1998. Adsorption characteristics of phenolic compounds onto coal-reject-derived adsorbents. Energy Fuel 12 (6), 1100–1107.
Hongo, T., Tsunashima, Y., Yamasaki, A., 2017. Synthesis of Ca-Al layered double hydroxide from concrete sludge and evaluation of its chromate removal ability. Sustain. Mater. Technol. 12, 23–26.
Inacio, J., Taviot-Gueho, C., Forano, C., Besse, J.P., 2001. Adsorption of MCPA pesticide by MgAl-layered double hydroxides. Appl. Clay Sci. 18 (5–6), 255–264.
Jain, N., Garg, M., 2008. Effect of Cr (VI) on the hydration behavior of marble dust blended cement: solidification, leachability and XRD analyses. Constr. Build. Mater. 22 (8), 1851–1856.
JCPD, 1995. Joint Committee on Power Diffraction Standard-International Centre forDiffraction Data. Swarthmore, PA.
Katsioti, M., Katsiotis, N., Rouni, G., Bakirtzis, D., Loizidou, M., 2008. The effect of bentonite/cement mortar for the stabilization/solidification of sewage sludge containing heavy metals. Cement & Concrete Composites 30 (10), 1013–1019.
Ke, X., Bernal, S.A., Provis, J.L., 2016. Controlling the reaction kinetics of sodium carbonate-activated slag cements using calcined layered double hydroxides. Cem. Concr. Res. 81, 24–37.
Lasheras-Zubiate, M., Navarro-Blasco, I., Álvarez, J.I., Fernández, J.M., 2011. Interaction of carboxymethylchitosan and heavy metals in cement media. Journal of hazardous Materials 194 (Supplement C), 223–231.
Lasheras-Zubiate, M., Navarro-Blasco, I., Fernandez, J.M., Alvarez, J.I., 2012. Encapsulation, solid-phases identification and leaching of toxic metals in cement systems modified by natural biodegradable polymers. J. Hazard. Mater. 233, 7–17.
Ledesma, E.F., Jimenez, J.R., Ayuso, J., Fernandez, J.M., de Brito, J., 2017. Experimental study of the mechanical stabilization of electric arc furnace dust using fluid cement mortars. J. Hazard. Mater. 326, 26–35.
Ledesma, E.F., Lozano-Lunar, A., Ayuso, J., Galvín, A.P., Fernández, J.M., Jiménez, J.R., 2018. The role of pH on leaching of heavy metals and chlorides from electric arc furnace dust in cement-based mortars. Constr. Build. Mater. 183, 365–375.
Li, F., Duan, X., 2006. Applications of layered double hydroxides, layered double hydroxides. Springer, pp. 193–223.
Liang, X., Zang, Y., Xu, Y., Tan, X., Hou, W., Wang, L., Sun, Y., 2013. Sorption of metal cations on layered double hydroxides. Colloids Surf. A Physicochem. Eng. Asp. 433, 122–131.
Lozano-Lunar, A., Fernández Ledesma, E., Romero Esquinas, Á., Jiménez Romero, J.R., Fernández Rodríguez, J.M., 2019a. A Double barrier technique with hydrotalcites for Pb immobilisation from electric arc furnace dust. Materials 12 (4), 633.
Lozano-Lunar, A., Raposeiro da Silva, P., de Brito, J., Fernández, J.M., Jiménez, J.R., 2019b. Safe use of electric arc furnace dust as secondary raw material in self-compacting mortars production. J. Clean. Prod. 211, 1375–1388.
Mol, S., 2011. Levels of Heavy Metals in Canned Bonito, Sardines, and Mackerel Produced in Turkey. Biol. Trace Elem. Res. 143 (2), 974–982.
Moon, G.D., Oh, S., Jung, S.H., Choi, Y.C., 2017. Effects of the fineness of limestone powder and cement on the hydration and strength development of PLC concrete. Constr. Build. Mater. 135, 129–136.
Navarro, A., Cardellach, E., Corbella, M., 2011. Immobilization of Cu, Pb and Zn in mine-contaminated soils using reactive materials. J. Hazard. Mater. 186 (2–3), 1576–1585.
Navarro-Blasco, I., Duran, A., Sirera, R., Fernandez, J.M., Alvarez, J.I., 2013. Solidification/stabilization of toxic metals in calcium aluminate cement matrices. J. Hazard. Mater. 260, 89–103.
Navarro-Blasco, I., Duran, A., Perez-Nicolas, M., Fernandez, J.M., Sirera, R., Alvarez, J.I., 2015. A safer disposal of hazardous phosphate coating sludge by formation of an amorphous calcium phosphate matrix. J. Environ. Manag. 159, 288–300.
Nestle, N., 2004. NMR relaxometry study of cement hydration in the presence of different oxidic fine fraction materials. Solid State Nucl. Magn. Reson. 25 (1–3), 80–83.
Otero, R., Fernández, J.M., Ulibarri, M.A., Celis, R., Bruna, F., 2012. Adsorption of non-ionic pesticide S-Metolachlor on layered double hydroxides intercalated with dodecylsulfate and tetradecanedioate anions. Appl. Clay Sci. 65-66, 72–79.
Otero, R., Fernández, J.M., González, M.A., Pavlovic, I., Ulibarri, M.A., 2013. Pesticides adsorption–desorption on Mg–Al mixed oxides. Kinetic modeling, competing factors and recyclability. Chem. Eng. J. 221, 214–221.
Otomoso, O., Ivey, D., Mikula, R., 1995. Electron microscopic and 29Si-nuclear magnetic resonance spectroscopic studies of chromium doped tricalcium silicate. In: Hager, J. P., Mishra, B., Davidson, C.F., Litz, J.L. (Eds.), Treatment and Minimisation of Heavy Metal-containing Wastes, 129.
Pensaert, S., Zwaenepoel, J., Vanhove, B., Dewilde, J., De Naeyer, F., Helmholtz Centre Environmental, R.-U., 2008. Case-study of the first remediation in Flanders by means of on-site immobilization on a heavy metal impacted site. Consoil 2008: Theme E - Remediation Concepts & Technologies, 1-3, pp. 667–672.
Pérez, M.R., Barriga, C., Fernández, J.M., Rives, V., Ulibarri, M.A., 2007. Synthesis of Cd/(Al+Fe) layered double hydroxides and characterization of the calcination products. J. Solid State Chem. 180 (12), 3434–3442.
Pérez, M.R., Crespo, I., Ulibarri, M.A., Barriga, C., Rives, V., Fernández, J.M., 2012. Influence of divalent metal on the decomposition products of hydrotalcite-like ternary systems MII–Al–Cr (MII=Zn, Cd). Mater. Chem. Phys. 132 (2), 375–386.
Pérez, A., Otero, R., Romero Esquinas, A., Jiménez, J.R., Fernández, J.M., 2017. Potential use of modified hydrotalcites as adsorbent of Bentazon and Metazachlor. Appl. Clay Sci. 141, 300–307.
Quina, M.J., Bordado, J.C.M., Quinta-Ferreira, R.M., 2014. Stabilisation/solidification of APC residues from MSW incineration with hydraulic binders and chemical additives. Journal of hazardous Materials 264 (Supplement C), 107–116.
Rouahna, N., Barkat, D., Ouakouak, A., Srasra, E., 2018. Synthesis and characterization of Mg-Al layered double hydroxide intercalated with D2EHPA: Application for copper ions removal from aqueous solution. Journal of Environmental Chemical Engineering 6 (1), 1226–1232.
Scrivener, K.L., Juilland, P., Monteiro, P.J.M., 2015. Advances in understanding hydration of Portland cement. Cem. Concr. Res. 78, 38–56.
Senff, L., Barbetta, P.A., Repette, W.L., Hotza, D., Paiva, H., Ferreira, V.M., Labrincha, J. A., 2009. Mortar composition defined according to rheometer and flow table tests using factorial designed experiments. Constr. Build. Mater. 23 (10), 3107–3111.
Shao, H.-F., Liu, C.-S., Huang, Y., Cao, X.-H., Yang, H.-C., 2001. Shape control of hydroxyapaptite crystal seed and its effects on the in-situ reinforcement of calcium phosphate cement. Journal of Inorganic Materials-Beijing 16 (5), 933–939.
Shui, Z.H., Yu, R., Chen, Y.X., Duan, P., Ma, J.T., Wang, X.P., 2018. Improvement of concrete carbonation resistance based on a structure modified Layered Double Hydroxides (LDHs): experiments and mechanism analysis. Constr. Build. Mater. 176, 228–240.
Sinyoung, S., Songsiriritthigul, P., Asavapisit, S., Kajitvichyanukul, P., 2011. Chromium behavior during cement-production processes: a clinkerization, hydration, and leaching study. J. Hazard. Mater. 191 (1–3), 296–305.
Tan, X., Wang, X., Fang, M., Chen, C., 2007. Sorption and desorption of Th(IV) on nanoparticles of anatase studied by batch and spectroscopy methods. Colloids Surf. A Physicochem. Eng. Asp. 296 (1), 109–116.
Theiss, F.L., Ayoko, G.A., Frost, R.L., 2016. Synthesis of layered double hydroxides containing Mg^{2+}, Zn^{2+}, Ca^{2+} and Al^{3+} layer cations by co-precipitation methods—a review. Appl. Surf. Sci. 383, 200–213.
Thomas, N.L., Jameson, D.A., Double, D.D., 1981. The effect of lead nitrate on the early hydration of Portland cement. Cem. Concr. Res. 11 (1), 143–153.
Thongsanitgarn, P., Wongkeo, W., Chaipanich, A., Poon, C.S., 2014. Heat of hydration of Portland high-calcium fly ash cement incorporating limestone powder: effect of limestone particle size. Constr. Build. Mater. 66, 410–417.
Villa, M.V., Sanchez-Martin, M.J., Sanchez-Camazano, M., 1999. Hydrotalcites and organo-hydrotalcites as sorbents for removing pesticides from water. Journal of Environmental Science and Health Part B-Pesticides Food Contaminants and Agricultural Wastes 34 (3), 509–525.
Wang, Q., O'Hare, D., 2012. Recent advances in the Synthesis and Application of Layered Double Hydroxide (LDH) Nanosheets. Chem. Rev. 112 (7), 4124–4155.
Wang, S., Vipulanandan, C., 2000. Solidification/stabilization of Cr (VI) with cement: Leachability and XRD analyses. Cem. Concr. Res. 30 (3), 385–389.
Weeks, C., Hand, R.J., Sharp, J.H., 2008. Retardation of cement hydration caused by heavy metals present in ISF slag used as aggregate. Cem. Concr. Compos. 30 (10), 970–978.
Wu, Y., Duan, P., Yan, C., 2018. Role of layered double hydroxides in setting, hydration degree, microstructure and compressive strength of cement paste. Appl. Clay Sci. 158, 123–131.
Xie, T., Biernacki, J.J., 2011. The origins and evolution of cement hydration models, p. 8.
Xu, S., Chen, Z., Zhang, B., Yu, J., Zhang, F., Evans, D.G., 2009. Facile preparation of pure CaAl-layered double hydroxides and their application as a hardening accelerator in concrete. Chem. Eng. J. 155 (3), 881–885.
Yang, Z.X., Fischer, H., Polder, R., 2015. Laboratory investigation of the influence of two types of modified hydrotalcites on chloride ingress into cement mortar. Cement & Concrete Composites 58, 105–113.
Yoon, S., Moon, J., Bae, S., Duan, X., Giannelis, E.P., Monteiro, P.M., 2014. Chloride adsorption by calcined layered double hydroxides in hardened Portland cement paste. Mater. Chem. Phys. 145 (3), 376–386.
Yousuf, M., Mollah, A., Vempati, R.K., Lin, T.C., Cocke, D.L., 1995. The interfacial chemistry of solidification/stabilization of metals in cement and pozzolanic material systems. Waste Manag. 15 (2), 137–148.